Resource Allocation for Multi-Cluster NOMA-UAV Networks

Qiulei Huang, Wei Wang, Weidang Lu, *Senior Member, IEEE,* Nan Zhao, *Senior Member, IEEE,* Arumugam Nallanathan, *Fellow, IEEE,* and Xianbin Wang, *Fellow, IEEE*

***Abstract*—Combining non-orthogonal multiple access (NOMA) and unmanned aerial vehicles (UAVs) could achieve better performance for wireless networks. However, effective resource allocation for quality of service (QoS) provision among all users still remains as a great challenge for multi-cluster NOMA-UAV networks. In this paper, we propose a NOMA-UAV scheme, where a UAV is deployed as the mobile base station to serve ground users. To meet the QoS requirements of all users with limited resource, the user clustering and optimal routing are first developed by the K-means algorithm and genetic algorithm, respectively. Then, the sum throughput is maximized by jointly optimizing the transmission power, hovering locations and transmission duration of UAV. To solve this non-convex problem with coupled variables, we decompose it into three subproblems. Among them, the power and location optimizations are also non-convex, which can be transformed into convex ones by successive convex approximation. The duration optimization is a linear programming which can be solved directly. Then, we propose an iterative algorithm to solve these three subproblems alternately. Finally, simulation results are presented to show the effectiveness of the proposed scheme.**

***Index Terms*—Genetic algorithm, K-means, non-orthogonal multiple access, resource allocation, unmanned aerial vehicle.**

I. Introduction

Recently, unmanned aerial vehicle (UAV) assisted wireless communication has become an important supplement to the terrestrial networks. On one hand, UAVs can be deployed flexibly due to the mobility [2], and thus, UAV-assisted communication is an effective solution for emergency communications without infrastructure [3]. On the other hand, the UAV-to-ground channels can be approximated as the high-quality line-of-sight (LoS) links [4]. Owing to these advantages, UAV-assisted communications have attracted great attentions from both academia and industry [5]–[7]. In [5], Gupta *et al.* identified the main challenges for UAV-assisted wireless networks. The channel models of UAV-aided communications were studied by Lin *et al.* in [6]. In [7], Zeng *et al.* introduced how to integrate UAVs into the fifth-generation and future wireless networks. However, the operation life of UAV is limited, due to the finite onboard energy. For this reason, how to allocate the resource effectively still remains a great challenge for UAV-assisted communications [8]–[11]. In [8], Zeng *et al.* deployed UAVs as the relaying nodes to maximize the system throughput by iteratively optimizing the power allocation and UAV trajectory. The minimum throughput of all ground users was maximized by Wu *et al.* via jointly adjusting the multi-user scheduling and UAV trajectory in [9]. In [10], Wang *et al.* proposed an effective algorithm to improve the throughput by jointly optimizing the transmission power and trajectory. In [11], the UAV trajectory and resource allocation were optimized by Wu and Zhang to maximize the minimum average throughput. In [12], Meng *et al.* jointly adjusted the UAV trajectory, transmit precoder and sensing start instant to maximize the achievable rate in UAV-enabled integrated sensing and communication systems.

On the other hand, non-orthogonal multiple access (NOMA) is becoming a promising technology to satisfy the requirements of super-high rate, ultra-low latency, ultra-reliability and massive connectivity [13]. In the power-domain NOMA, more power will be allocated to the users with worse channels to allow them to share the same resource block [14]. Then, the high-power signals are first decoded and removed via successive interference cancellation (SIC) before decoding the lower ones. In [15], Liu *et al.* presented the current research efforts and future application scenarios for NOMA. Ding *et al.* proposed two NOMA-assisted caching strategies to provide additional bandwidth in [16]. In [17], Chen *et al.* proved that NOMA can always achieve better performance than orthogonal multiple access (OMA) when both have the optimal resource allocation policies. However, there exists serious interference between users because they share the same resource block. Thus, the power allocation is extremely significant for NOMA systems [18]–[22]. In [18], Wang *et al*. proposed a power allocation scheme to maximize the sum capacity for single-input single-output NOMA system with two users. Yang *et al.* adopted power control for multi-cell downlink NOMA networks to minimize the sum power while maximizing the sum rate in [19]. In [20], Xiao *et al.* maximized the sum rate for millimeter-wave NOMA communications by jointly optimizing the transmission power and beamforming. The transmission rate was maximized by Zhu *et al.* through jointly optimizing the transmission power and beamforming for uplink NOMA in [21]. In [22], Feng *et al.* designed a power allocation algorithm, which adopts NOMA to maximize the sum throughput.

Q. Huang, W. Wang and N. Zhao are with the School of Information and Communication Engineering, Dalian University of Technology, Dalian 116024, China. (email: qiuleihuang@mail.dlut.edu.cn; 21809066@mail.dlut.edu.cn; zhaonan@dlut.edu.cn).

W. Lu is with the College of Information Engineering, Zhejiang University of Technology, Hangzhou 310058, China (e-mail: luweid@zjut.edu.cn).

Arumugam Nallanathan is with the School of Electronic Engineering and Computer Science, Queen Mary University of London, London WC1E 7HU, U.K. (e-mail: a.nallanathan@qmul.ac.uk)

X. Wang is with the Department of Electrical and Computer Engineering, Western University, London, ON, Canada (e-mail: xianbin.wang@uwo.ca).

Part of this paper will be presented at IEEE GLOBECOM 2022 [1].

(Corresponding author: Nan Zhao.)

Due to their own advantages, it is natural to integrate NOMA into UAV-assisted communications to further improve the performance [23]–[26]. Zhao *et al.* proposed an effective algorithm in [23] to maximize the sum rate via jointly adjusting the trajectory and NOMA precoding. In [24], Liu *et al.* proposed a unified framework to study the UAV-aided networks with massive access capability supported by NOMA. In [25], the sum rate was maximized by Liu *et al.* through jointly optimizing the location of UAV and the transmission power for NOMA-UAV networks. Furthermore, the decoding order was considered by Zhang *et al.* in [26] to achieve better performance than the scheme in [25].

When there are more users to be served by the UAV, only a single NOMA group cannot accommodate all of them, and we should divide them into multiple clusters. Accordingly, NOMA can be utilized in each cluster. However, to the best of our knowledge, the resource allocation design for NOMA-UAV networks with multiple clusters has not been fully investigated, and only a few literatures have focused on this direction [27], [28]. In [27], the sum rate was maximized by Feng *et al.* through jointly adjusting the three-dimensional locations of UAV, beam pattern and transmission power, where the optimal UAV routing was obtained by the branch and bound algorithm. In [28], Katwe *et al.* deployed multiple UAVs to improve the sum rate of the NOMA-UAV system by dynamic user clustering, optimal UAV placement and power allocation, where each cluster was served by a single UAV.

Inspired by the above-mentioned works, in this paper, we propose a resource allocation scheme to maximize the sum throughput for multi-cluster NOMA-UAV networks. Different from [27] and [28], the users are first clustered by the K-means algorithm. To reduce the computational complexity, the UAV routing is obtained by the genetic algorithm. In addition, the decoding order and global impact are also considered to improve the performance when optimizing the transmission power, hovering locations and transmission duration. In summary, the main motivations and contributions of this paper are as follows:

- A new effective multi-cluster scheme for NOMA-UAV networks is proposed to satisfy the quality of service (QoS) of all the users with limited resource. The sum throughput of the network is maximized by optimizing the user clustering, UAV routing and hovering locations, SIC decoding order, transmission power as well as duration allocation.
- A NOMA clustering algorithm is first developed by the K-means algorithm to support the proposed multi-cluster scheme, which are closely related to the distribution of user positions. Accordingly, the UAV routing optimization with multiple clusters can be deemed as a traveling salesman problem (TSP), and we propose a GA-based algorithm to solve it, which can greatly decrease the computational complexity.
- Based on the optimized user clustering and UAV routing, the sum throughput maximization problem is decomposed into three subproblems of transmission power, hovering locations and transmission duration, which can be transformed into convex ones by successive convex approximation (SCA). Then, we propose an iterative algorithm to solve these subproblems alternately.

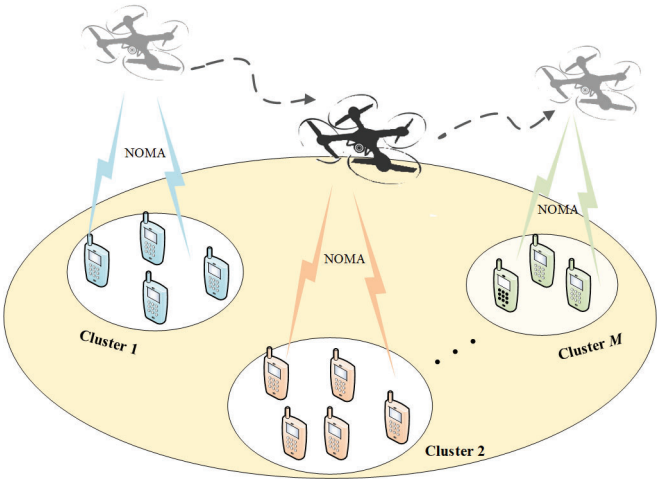

Fig. 1. A K-user NOMA-UAV network with M clusters.

The rest of this paper is organized as follows. In Section II, the system model is presented. User clustering and UAV routing are optimized in Section III. In Section IV, the sum throughput is maximized by jointly optimizing the locations, power and duration. Simulation results and discussion are shown in Section V, followed by the conclusion in Section VI.

Notation: $\|\mathbf{L}\|$ and $\mathbf{L}^{\dagger}$ denote the Euclidean norm and transpose matrix of $\mathbf{L}$. $\mathbb{R}^{2\times 1}$ is the space of 2×1 matrices. $\bigtriangledown f(x)$ represents the gradient function of $f(x)$. The factorial of M is denoted as $M!$.

II. System Model

Consider a NOMA-UAV network where a UAV is deployed as the mobile base station (BS) with a single antenna to serve K single-antenna ground users as shown in Fig. 1. The users are assumed to be divided into M clusters. Define the set of clusters as $\mathbf{\Lambda} = \{1, 2, ..., M\}$. There are N_m users in the m-th cluster. The set of users in the m-th cluster is defined as $\mathbf{\Gamma_m} = \{1, 2, ..., N_m\}, m \in \mathbf{\Lambda}$. Thus, we have

$$K = \sum_{m=1}^{M} N_m, m \in \mathbf{\Lambda}. \tag{1}$$

The UAV takes off from the initial point, and sequentially flies to the hovering point of each cluster according to the predefined trajectory. The transmission is performed only when hovering to avoid the Doppler effect. Meanwhile, to achieve high spectrum efficiency and massive connections, the UAV serves the users in each cluster via NOMA.

The whole duration T_0 can be divided into the flying duration T_S and the transmission duration. The transmission duration for the m-th cluster is denoted as τ_m. Thus, we have

$$\sum_{m=1}^{M} \tau_m + T_S \leq T_0. \tag{2}$$

Denote the n-th user in the m-th cluster as $U_{m,n}$. The distance from the UAV to $U_{m,n}$ when connected can be represented by $d_{m,n}$. Assume that the UAV is flying at the altitude H_0. Define the horizontal hovering coordinate of the UAV for the m-th cluster as $\mathbf{L}_m = [A_m, B_m]^\dagger \in \mathbb{R}^{2\times 1}$, and the position of $U_{m,n}$ as $\mathbf{q}_{m,n} = [a_{m,n}, b_{m,n}]^\dagger \in \mathbb{R}^{2\times 1}$. Therefore, $d_{m,n}$ can be calculated as

$$d_{m,n} = \sqrt{H_0^2 + \parallel \mathbf{q}_{m,n} - \mathbf{L}_m \parallel^2}, n \in \boldsymbol{\Gamma_m}, m \in \boldsymbol{\Lambda}. \quad (3)$$

Without loss of generality, in the m-th cluster, we assume

$$d_{m,1} \leq d_{m,2} \leq \cdots \leq d_{m,N_m}. \quad (4)$$

Define $h_{m,n}$ as the channel coefficient from the UAV to $U_{m,n}$. According to [29], the LoS probability is almost 1 when the UAV is higher than a suitable altitude, e.g., 120 m. Thus, the air-ground channels can be approximated as LoS, which is expressed as

$$\mid h_{m,n} \mid^2 = \rho_0 d_{m,n}^{-2}, \quad (5)$$

where ρ_0 is the reference channel coefficient of the unit distance 1 m.

According to NOMA, SIC is adopted at the receivers to guarantee the fairness among users, and the user with weaker channel will be compensated for more transmission power. Define $P_{m,n}$ as the transmission power for $U_{m,n}$. Thus, according to the distance order in (4), $P_{m,n}$ should satisfy

$$0 < P_{m,1} \leq P_{m,2} \leq ... \leq P_{m,N_m}. \quad (6)$$

Meanwhile, the sum transmission power for all the users in each cluster should not exceed the power limit of UAV P_{sum}, and we have

$$\sum_{n=1}^{N_m} P_{m,n} \leq P_{sum}. \quad (7)$$

Therefore, the received signal at $U_{m,i}$ can be expressed as

$$y_{m,i} = h_{m,i} \sum_{j=1}^{N_m} \sqrt{P_{m,j}} x_{m,j} + n_{m,i}, \quad (8)$$

where $n_{m,i}$ represents the additive white Gaussian noise (AWGN) with variance σ^2 and zero mean at $U_{m,i}$, and $x_{m,i}$ denotes the message of $U_{m,i}$ with the unit power of $|x_{m,i}|^2 = 1$.

In NOMA, each user first decodes the stronger signals and removes them from the superposed signal before decoding its own. Thus, according to (4), the signal-to-interference-plus-noise ratio (SINR) for $U_{m,n}$ can be denoted as

$$\mathrm{SINR}_{m,n} = \frac{|h_{m,n}|^2 P_{m,n}}{|h_{m,n}|^2 \sum_{j=1}^{n-1} P_{m,j} + \sigma^2}, 2 \leq n \leq N_m. \quad (9)$$

In particular, when $n = 1$, the SINR can be denoted as

$$\mathrm{SINR}_{m,1} = \frac{|h_{m,1}|^2 P_{m,1}}{\sigma^2}. \quad (10)$$

In addition, the messages from weaker users should be also correctly decoded at the receiver with better channel. Thus, we have the constraint as

$$\mathrm{SINR}_{m,n}^{min} = \min\{\mathrm{SINR}_{m,n}^1, \cdots, \mathrm{SINR}_{m,n}^n\} \geq \eta_{m,n}, \quad (11)$$

Algorithm 1 - K-means Algorithm for user clustering

1: **Initialization**: Randomly select M users as the initial centroids.
2: **Repeat**
3: For each user, calculate the Euclidean distance from it to each centroid.
4: Each user can be assigned to the cluster with the shortest distance from it.
5: Update the centroids by (14).
6: **Until** the centroids no longer change.
7: Output: $\boldsymbol{\Gamma_m}, \forall m \in \Lambda$.

where $\eta_{m,n}$ is the QoS requirement of $U_{m,n}$. Define $\mathrm{SINR}_{m,n}^w, \{w \leq n \in \boldsymbol{\Gamma_m}\}$ as the SINR when the signal of $U_{m,n}$ is decoded at the receiver $U_{m,w}$, which can be expressed as

$$\mathrm{SINR}_{m,n}^w = \frac{|h_{m,w}|^2 P_{m,n}}{|h_{m,w}|^2 \sum_{j=1}^{n-1} P_{m,j} + \sigma^2}, w \leq n. \quad (12)$$

In particular, $\mathrm{SINR}_{m,n}^w = \mathrm{SINR}_{m,n}$ when $w = n$.

Accordingly, the downlink achievable rate of $U_{m,n}$ can be denoted as

$$R_{m,n} = \log_2(1 + \mathrm{SINR}_{m,n}^{min}). \quad (13)$$

III. Clustering and Routing Optimization

As the available resource of UAV is limited, the user clustering and UAV flying route should be scheduled properly. To this end, we first utilize the K-means algorithm for user clustering in this section, and then propose a GA-based algorithm to optimize the UAV routing.

A. User Clustering Optimization

In the network, the ground users locate in the distribution of clusters. Thus, the K-means algorithm can be adopted to realize the user clustering, which is an effective method with fast convergence. The specific algorithm is described as follows.

At first, we select M initial centroids randomly, with the centroid of the m-th cluster defined as $\boldsymbol{\mu}_m$. Calculate the distances from the users to each centroid. Each user is organized into the cluster whose centroid is closest to it. After all the users have been assigned, $\boldsymbol{\mu}_m$ can be updated as

$$\boldsymbol{\mu}_m = \frac{1}{N_m} \sum_{n=1}^{N_m} \mathbf{q}_{m,n}. \quad (14)$$

Then, the users are organized again according to the new centroids. The above steps are iteratively carried out until convergence [30]. The details of the proposed K-means algorithm are described in Algorithm 1.

To further improve the performance, choosing a proper M is important for the K-means algorithm. Thus, we introduce the sum of the squared errors as

$$\mathcal{J} = \sum_{m=1}^{M} \sum_{n=1}^{N_m} \|\mathbf{q}_{m,n} - \boldsymbol{\mu}_m\|^2, \quad (15)$$

Algorithm 2 - GA for Routing Optimization

1: **Initialization**: Define the centroids of clusters as the initial hovering locations of UAV. Set the initial index of iterations as t = 1. Generate the initial generation with Z individuals.
2: **Repeat**
3: Calculate the fitness function $\psi^t(z)$ for each individual.
4: Find the individual with the largest fitness and decode the corresponding distance λ^t_{min} and route.
5: When $\lambda^t_{min} < S_{min}$, update $S_{min} = \lambda^t_{min}$ and $\mathbf{G}$ is the array of this individual.
6: **Repeat**
7: Generate ε_2 to select two ancestors.
8: Create the new route for the $(t+1)$-th iteration.
9: Generate ε_3.
10: Exchange the order of the two codes in this individual when $\varepsilon_3 \leq \varrho$.
11: **Until** the new routes are enough.
12: Update: $t = t + 1$.
13: **Until** $t = \beta$.
14: **Output**: $\mathbf{G}$ and S_{min}.

which always decreases with the increase of M. A smaller value of $\mathcal{J}$ means that the result of clustering is better. However, the clustering becomes ineffective when M gets close to K. Thus, we adopt the elbow method to obtain the proper M [31], in which the K-means algorithm is performed with different M. $\mathcal{J}$ decreases sharply before the elbow when M increases, after which the trend becomes stable. We can set this elbow as the proper value of M, which will be further demonstrated in Section V.

B. Routing Optimization

After the clusters are determined, we should find the optimal routing, which reflects the shortest flying distance for the UAV. The routing optimization can be deemed as a TSP. Generally, the optimal routing with M clusters can be obtained by the exhaustive search (ES), the computational complexity of which is $\mathcal{O}(M!)$. However, the complexity of ES becomes extremely high when the number of clusters increases. Thus, we propose a GA-based routing optimization algorithm, which can be described as follows.

1) *Encoding*: Assume that there are Z individuals in the t-th iteration, the set of which is defined as $\Omega^t = \{1, 2, \cdots, Z\}$. Each individual represents a UAV routing, which can be encoded as an array including the initial point and the cluster numbers from 1 to M. The index number of the initial point is set as 0, which locates at $\mathbf{L}_0 = (0, 0)$. We define the array $\mathbf{G}^t_z$ as the z-th individual in the t-th iteration. Thus, its distance $\lambda^t(z)$ can be calculated by

$$\lambda^t(z) = \sum_{i=1}^{M} \parallel \mathbf{L}_{\mathbf{G}^t_z(i+1)} - \mathbf{L}_{\mathbf{G}^t_z(i)} \parallel, z \in \Omega^t. \tag{16}$$

2) *Fitness Function*: The fitness function is crucial for the GA algorithm to evaluate the routes. Thus, the fitness function can be expressed as

$$\psi^t(z) = \frac{\lambda^t_{max} - \lambda^t(z) + \varepsilon_1}{\lambda^t_{max} - \lambda^t_{min} + \varepsilon_1}, \tag{17}$$

where λ^t_{max} and λ^t_{min} are the maximum and minimum distance in the t-th iteration, respectively. Meanwhile, we introduce a constant ε_1 to guarantee that the denominator of (17) is not equal to 0. Larger value of this function means that the corresponding route is better.

3) *Ancestor Selecting*: To generate the new routes for the next iteration, we need to select the individuals in the current iteration as ancestors via the roulette wheel selection. First, the cumulative probability of the z-th individual in the t-th iteration can be calculated as

$$\varphi^t(z) = \sum_{i=1}^{z} \frac{\psi^t(i)}{\sum_{j=1}^{Z} \psi^t(j)}, z \in \Omega^t. \tag{18}$$

Then, a random $\varepsilon_2 \in (0, 1]$ is generated. The z-th individual is selected as the ancestor when $\varphi^t(z-1) < \varepsilon_2 \leq \varphi^t(z)$. Repeat the operations until enough ancestors can be generated.

4) *Creating New Routes*: When creating the new routes, mutation is needed to avoid local optimums. Define ϱ as the mutation probability. The specific steps are as follows. First, a part of elements in an ancestor array is selected as the corresponding elements of the new route. Meanwhile, organize the rest elements of this route array according to the order of another ancestor's elements. Then, generate a random $\varepsilon_3 \in (0, 1)$. When $\varepsilon_3 \leq \varrho$, randomly exchange the order of the two elements in the new route.

Define the maximum number of iterations as β. Assume that the optimal routing is stored in a $(M+1) \times 1$ matrix $\mathbf{G}$. The shortest distance is denoted by S_{min}, which can be calculated by (16). The specific steps of GA are shown in Algorithm 2. The computational complexity of GA can be calculated by $\mathcal{O}(Z\beta M^2)$, which is dominated by creating the new routes [32]. Compared with the ES, the proposed GA-based algorithm can greatly decrease the computational complexity with the increasing number of clusters.

IV. Optimization for Maximizing Throughput

In this section, the resource of UAV is allocated based on the user clustering and routing optimization in Section III. We first formulate the problem of resource allocation, which is non-convex. Then, we decompose it into three subproblems. In the end, an effective algorithm is proposed to solve the subproblems alternately.

A. Problem Formulation

To take the full advantage of the resource, we aim at maximizing the system throughput by jointly optimizing the transmission power $\mathbf{P} = \{P_{m,n} | n \in \mathbf{\Gamma_m}, m \in \mathbf{\Lambda}\}$, the UAV hovering locations $\mathbf{L} = \{\mathbf{L}_m | m \in \mathbf{\Lambda}\}$ and the transmission duration allocation $\mathbf{T} = \{\tau_m | m \in \mathbf{\Lambda}\}$. Thus, the optimization

problem can be formulated as

$$
\begin{aligned}
(\mathrm{P1}): \max_{\mathbf{P},\mathbf{L},\mathbf{T}} & \sum_{m=1}^{M}\sum_{n=1}^{N_m} R_{m,n}\tau_m \\
s.t. & \sum_{m=1}^{M}\tau_m + T_S \le T_0, && \text{(19a)}\\
& R_{m,n}\tau_m \ge \delta_{m,n}, && \text{(19b)}\\
& \mathrm{SINR}_{m,n}^{min} \ge \eta_{m,n}, n \in \mathbf{\Gamma_m}, m \in \mathbf{\Lambda}, && \text{(19c)}\\
& 0 < P_{m,1} \le P_{m,2} \le ... \le P_{m,N_m}, && \text{(19d)}\\
& \sum_{n=1}^{N_m} P_{m,n} \le P_{sum}, && \text{(19e)}\\
& \sum_{i=1}^{M} \|\mathbf{L}_{\mathbf{G}(i+1)} - \mathbf{L}_{\mathbf{G}(i)}\| \le S_{min}. && \text{(19f)}
\end{aligned}
$$

In (P1), (19a) defines the whole duration of UAV, including the flying and transmission duration. (19b) ensures that the throughput for $U_{m,n}$ should exceed a threshold $\delta_{m,n}$. The QoS of each user is guaranteed by (19c). (19d) restricts the power allocation according to the distance order in (4). The sum transmission power is limited by (19e). (19f) ensures that the flying distance cannot ascend with the change of hovering locations.

(P1) is a non-convex problem with $\mathbf{P}, \mathbf{L}$ and $\mathbf{T}$ coupled, which is difficult to solve directly. To simplify (P1), we decompose it into three subproblems, i.e., the transmit power optimization, the hovering location optimization and the duration optimization. Among them, both the power and location optimization are non-convex, which can be transformed into convex ones via the first order Taylor approximation. The duration optimization is a linear programming, which can be solved directly. In the end, we propose an effective algorithm to solve these three subproblems iteratively.

B. Transmission Power Optimization

For any given UAV location $\mathbf{L}$ and transmission duration $\mathbf{T}$, (P1) can be decomposed as

$$
\begin{aligned}
\max_{\mathbf{P}} & \sum_{m=1}^{M}\sum_{n=1}^{N_m} R_{m,n}\tau_m \\
s.t.\ & R_{m,n}\tau_m \ge \delta_{m,n}, && \text{(20a)}\\
& \mathrm{SINR}_{m,n}^{min} \ge \eta_{m,n}, && \text{(20b)}\\
& 0 < P_{m,1} \le P_{m,2} \le ... \le P_{m,N_m}, && \text{(20c)}\\
& \sum_{n=1}^{N_m} P_{m,n} \le P_{sum}, n \in \mathbf{\Gamma_m}, m \in \mathbf{\Lambda}, && \text{(20d)}
\end{aligned}
$$

which is intractable due to the non-convex objective function and the constraints (20a) and (20b). Thus, SCA is adopted to approximate them as convex ones.

For the objective function and the constraints (20a), we have

$$
\begin{aligned}
R_{m,n} &= \log_2\left(1+\mathrm{SINR}_{m,n}^{min}\right) \\
&= \log_2\left(1+\min\{\mathrm{SINR}_{m,n}^{w}\}\right), w \le n \in \mathbf{\Gamma_m}, \qquad (21)
\end{aligned}
$$

where $\mathrm{SINR}_{m,n}^{min}$ can be obtained by Proposition 1.

Proposition 1: $\mathrm{SINR}_{m,n}^{min} = \mathrm{SINR}_{m,n}$.

Proof: $\mathrm{SINR}_{m,n}^{min} = \min\{\mathrm{SINR}_{m,n}^{w}\}$, and $\mathrm{SINR}_{m,n}^{w}$ can be rewritten as

$$
\begin{aligned}
\mathrm{SINR}_{m,n}^{w} &= \frac{|h_{m,w}|^2 P_{m,n}}{|h_{m,w}|^2 \sum_{j=1}^{n-1} P_{m,j} + \sigma^2} \\
&= \frac{P_{m,n}}{\sum_{j=1}^{n-1} P_{m,j} + \frac{\sigma^2}{|h_{m,w}|^2}}. \qquad (22)
\end{aligned}
$$

We can find that $\mathrm{SINR}_{m,n}^{w}$ increases with $|h_{m,w}|^2$, which is determined by the distance $d_{m,n}$. To be specific, the users with longer distance always have the worse channels. Thus, the users with larger index numbers have worse channels in each cluster according to the distance order in (4). Due to $w \le n$, we can obtain $\mathrm{SINR}_{m,n}^{min} = \mathrm{SINR}_{m,n}^{n} = \mathrm{SINR}_{m,n}$. ■

Substituting $\mathrm{SINR}_{m,n}^{min}$ by $\mathrm{SINR}_{m,n}$ in $R_{m,n}$, we can obtain

$$
\begin{aligned}
R_{m,n} &= \log_2\left(1+\frac{|h_{m,n}|^2 P_{m,n}}{|h_{m,n}|^2 \sum_{j=1}^{n-1} P_{m,j} + \sigma^2}\right) \\
&= \log_2\left(\frac{|h_{m,n}|^2 \sum_{j=1}^{n} P_{m,j} + \sigma^2}{|h_{m,n}|^2 \sum_{j=1}^{n-1} P_{m,j} + \sigma^2}\right), 2 \le n \le N_m, \qquad (23)
\end{aligned}
$$

which can be expanded as

$$
\begin{aligned}
R_{m,n} &= \log_2\left(|h_{m,n}|^2 \sum_{j=1}^{n} P_{m,j} + \sigma^2\right) \\
&\quad - \log_2\left(|h_{m,n}|^2 \sum_{j=1}^{n-1} P_{m,j} + \sigma^2\right). \\
&= \widetilde{R}_{m,n} - \overline{R}_{m,n}. \qquad (24)
\end{aligned}
$$

$R_{m,n}$ is a non-concave function with respect to $\mathbf{P}$ due to $\overline{R}_{m,n}$. Thus, we adopt the first-order Taylor expansion to approximate it.

Define $P_{m,n}^{r}$ as the transmission power of $U_{m,n}$ in the r-th iteration. Since $\overline{R}_{m,n}$ is concave, the first-order Taylor expansion of it at $P_{m,n}^{r}$ can be deduced as

$$
\begin{aligned}
\overline{R}_{m,n} &= \log_2\left(|h_{m,n}|^2 \sum_{j=1}^{n-1} P_{m,j} + \sigma^2\right) \\
&\le \sum_{j=1}^{n-1} \frac{|h_{m,n}|^2 \log_2(e)}{|h_{m,n}|^2 \sum_{j=1}^{n-1} P_{m,j}^{r} + \sigma^2}\left(P_{m,j} - P_{m,j}^{r}\right) \\
&\quad + \log_2\left(|h_{m,n}|^2 \sum_{j=1}^{n-1} P_{m,j}^{r} + \sigma^2\right) \triangleq \overline{R}_{m,n}^{[e]}, \qquad (25)
\end{aligned}
$$

which is approximated to a concave function. (20a) can be rewritten as

$$R_{m,n}\tau_m \geq \left(\widetilde{R}_{m,n} - \overline{R}^{[e]}_{m,n}\right)\tau_m \geq \delta_{m,n}, 2 \leq n \leq N_m. \quad (26)$$

In particular, when $n = 1$, $R_{m,1}$ needs to satisfy

$$R_{m,1}\tau_m = \log_2\left(1 + \frac{|h_{m,1}|^2 P_{m,1}}{\sigma^2}\right)\tau_m \geq \delta_{m,1}, \quad (27)$$

which is a concave constraint.

Then, according to Proposition 1, (20b) can be transformed as

$$\frac{|h_{m,n}|^2 P_{m,n}}{|h_{m,n}|^2 \sum_{j=1}^{n-1} P_{m,j} + \sigma^2} \geq \eta_{m,n}, \quad (28)$$

which can be rewritten into a convex constraint as

$$P_{m,n} - \eta_{m,n}\sum_{j=1}^{n-1} P_{m,j} \geq \frac{\sigma^2 \eta_{m,n}}{|h_{m,n}|^2}. \quad (29)$$

As a result, the problem (20) can be approximated as

$$\begin{aligned}
(\mathrm{P2}): \max_{\mathbf{P}} \; & \sum_{m=1}^{M}\sum_{n=1}^{N_m}\left(\widetilde{R}_{m,n} - \overline{R}^{[e]}_{m,n}\right)\tau_m \\
s.t. \; & \left(\widetilde{R}_{m,n} - \overline{R}^{[e]}_{m,n}\right)\tau_m \geq \delta_{m,n}, && (30a)\\
& P_{m,n} - \eta_{m,n}\sum_{j=1}^{n-1} P_{m,j} \geq \frac{\sigma^2\eta_{m,n}}{|h_{m,n}|^2}, && (30b)\\
& 0 < P_{m,1} \leq P_{m,2} \leq ... \leq P_{m,N_m}, && (30c)\\
& \sum_{n=1}^{N_m} P_{m,n} \leq P_{sum}, n \in \mathbf{\Gamma_m}, m \in \mathbf{\Lambda}, && (30d)
\end{aligned}$$

which is convex and can be solved by CVX.

C. Location Optimization

Then, with the fixed transmission power **P** and duration **T**, the hovering location can be optimized as

$$\begin{aligned}
\max_{\mathbf{L}} \; & \sum_{m=1}^{M}\sum_{n=1}^{N_m} R_{m,n}\tau_m \\
s.t. \; & \mathrm{SINR}^{min}_{m,n} \geq \eta_{m,n}, && (31a)\\
& R_{m,n}\tau_m \geq \delta_{m,n}, n \in \mathbf{\Gamma_m}, m \in \mathbf{\Lambda}, && (31b)\\
& \sum_{i=1}^{M} \|\mathbf{L}_{\mathbf{G}(i+1)} - \mathbf{L}_{\mathbf{G}(i)}\| \leq S_{min}. && (31c)
\end{aligned}$$

The objective function, (31a) and (31b) are non-convex with respect to **L**. First, for (31a), we introduce Proposition 2 to further handle it.

Proposition 2: (31a) can be transformed as

$$\|\mathbf{q}_{m,w} - \mathbf{L}_m\|^2 \leq \rho_0 \frac{P_{m,n} - \eta_{m,n}\sum_{j=1}^{n-1} P_{m,j}}{\eta_{m,n}\sigma^2} - H_0^2, w \leq n, \quad (32)$$

which is convex and can be solved directly.

Proof: $\mathrm{SINR}^{min}_{m,n}$ can be calculated as

$$\begin{aligned}
\mathrm{SINR}^{min}_{m,n} &= \min\{\mathrm{SINR}^{w}_{m,n}\}, w \leq n \\
&= \min\{\mathrm{SINR}^{1}_{m,n}, \cdots, \mathrm{SINR}^{n}_{m,n}\}. \quad (33)
\end{aligned}$$

To achieve (31a), we have

$$\begin{cases}
\mathrm{SINR}^{1}_{m,n} \geq \eta_{m,n}, \\
\mathrm{SINR}^{2}_{m,n} \geq \eta_{m,n}, \\
\quad \cdots \qquad\qquad , \\
\mathrm{SINR}^{n}_{m,n} \geq \eta_{m,n}.
\end{cases} \quad (34)$$

$\mathrm{SINR}^{w}_{m,n}$ needs to satisfy

$$\frac{\frac{\rho_0}{H_0^2 + \|\mathbf{q}_{m,w} - \mathbf{L}_m\|^2} P_{m,n}}{\frac{\rho_0}{H_0^2 + \|\mathbf{q}_{m,w} - \mathbf{L}_m\|^2}\sum_{j=1}^{n-1} P_{m,j} + \sigma^2} \geq \eta_{m,n}, w \leq n, \quad (35)$$

which can be rewritten as

$$\frac{\rho_0 P_{m,n}}{\rho_0 \sum_{j=1}^{n-1} P_{m,j} + \sigma^2\left(H_0^2 + \|\mathbf{q}_{m,w} - \mathbf{L}_m\|^2\right)} \geq \eta_{m,n}. \quad (36)$$

Thus, we have

$$\eta_{m,n}\sigma^2\left(H_0^2 + \|\mathbf{q}_{m,w} - \mathbf{L}_m\|^2\right) \leq \rho_0\left(P_{m,n} - \eta_{m,n}\sum_{j=1}^{n-1} P_{m,j}\right). \quad (37)$$

Accordingly, (32) can be derived. ■

Then, for (31b), we have

$$\begin{cases}
\log_2\left(1 + \mathrm{SINR}^{1}_{m,n}\right)\tau_m \geq \delta_{m,n}, \\
\log_2\left(1 + \mathrm{SINR}^{2}_{m,n}\right)\tau_m \geq \delta_{m,n}, \\
\quad \cdots \qquad\qquad , \\
\log_2\left(1 + \mathrm{SINR}^{n}_{m,n}\right)\tau_m \geq \delta_{m,n},
\end{cases} \quad (38)$$

which is non-convex. For convenience, we define $\log_2\left(1 + \mathrm{SINR}^{w}_{m,n}\right)$ as $R^{w}_{m,n}$. To perform the approximation, we rewrite $R^{w}_{m,n}$ as

$$\begin{aligned}
R^{w}_{m,n} &= \log_2\left(1 + \frac{|h_{m,w}|^2 P_{m,n}}{|h_{m,w}|^2 \sum_{j=1}^{n-1} P_{m,j} + \sigma^2}\right) \\
&= \hat{R}^{w}_{m,n} - \check{R}^{w}_{m,n}, w \leq n, m \in \mathbf{\Lambda}, \quad (39)
\end{aligned}$$

where $\hat{R}^{w}_{m,n}$ and $\check{R}^{w}_{m,n}$ can be expressed as

$$\begin{cases}
\hat{R}^{w}_{m,n} = \log_2\left(\frac{\rho_0}{H_0^2 + \|\mathbf{q}_{m,w} - \mathbf{L}_m\|^2}\sum_{j=1}^{n} P_{m,j} + \sigma^2\right), \\
\check{R}^{w}_{m,n} = \log_2\left(\frac{\rho_0}{H_0^2 + \|\mathbf{q}_{m,w} - \mathbf{L}_m\|^2}\sum_{j=1}^{n-1} P_{m,j} + \sigma^2\right).
\end{cases} \quad (40)$$

Regarding $\|\mathbf{q}_{m,w} - \mathbf{L}_m\|^2$ as a variable, we have that both $\hat{R}^{w}_{m,n}$ and $\check{R}^{w}_{m,n}$ are convex. Thus, we need to first transform $\hat{R}^{w}_{m,n}$ into a concave one. Define L^{r}_{m} as the hovering location

in the r-th iteration. We can obtain the first-order expansion of $\hat{R}^w_{m,n}$ at $\|\mathbf{q}_{m,w}-\mathbf{L}^r_m\|^2$ as

$$\begin{aligned}\hat{R}^w_{m,n} =& \log_2\left(\frac{\rho_0}{H_0^2+\|\mathbf{q}_{m,w}-\mathbf{L}_m\|^2}\sum_{j=1}^{n}P_{m,j}+\sigma^2\right)\\ \geq& -C^w_{m,n}\left(\|\mathbf{q}_{m,w}-\mathbf{L}_m\|^2-\|\mathbf{q}_{m,w}-\mathbf{L}^r_m\|^2\right)\\ &+\log_2\left(\frac{\rho_0}{H_0^2+\|\mathbf{q}_{m,w}-\mathbf{L}^r_m\|^2}\sum_{j=1}^{n}P_{m,j}+\sigma^2\right)\\ \triangleq& \dot{R}^w_{m,n},\end{aligned} \tag{41}$$

which is concave with respect to $\mathbf{L}$. $C^w_{m,n}$ can be expressed as

$$C^w_{m,n}=\frac{\frac{\rho_0\log_2(e)}{(H_0^2+\|\mathbf{q}_{m,w}-\mathbf{L}^r_m\|^2)^2}\sum_{j=1}^{n}P_{m,j}}{\frac{\rho_0}{H_0^2+\|\mathbf{q}_{m,w}-\mathbf{L}^r_m\|^2}\sum_{j=1}^{n}P_{m,j}+\sigma^2}. \tag{42}$$

Accordingly, $R^w_{m,n}$ can be approximated as

$$R^w_{m,n}\geq \dot{R}^w_{m,n}-\check{R}^w_{m,n}, \tag{43}$$

which is still non-concave with respect to $\mathbf{L}$ due to $\check{R}^w_{m,n}$. Therefore, we introduce the slack variable $V_{m,w}$, which satisfies

$$V_{m,w}\leq\|\mathbf{q}_{m,w}-\mathbf{L}_m\|^2, w\in\mathbf{\Gamma_m}, m\in\mathbf{\Lambda}. \tag{44}$$

This is a non-convex constraint due to $\|\mathbf{q}_{m,w}-\mathbf{L}_m\|^2$. Thus, we approximate it through the first-order expansion at L^r_m as

$$\|\mathbf{q}_{m,w}-\mathbf{L}_m\|^2\geq\|\mathbf{q}_{m,w}-\mathbf{L}^r_m\|^2+2(\mathbf{q}_{m,w}-\mathbf{L}^r_m)^\dagger(\mathbf{L}^r_m-\mathbf{L}_m). \tag{45}$$

As a result, for (44), we have

$$V_{m,w}\leq\|\mathbf{q}_{m,w}-\mathbf{L}^r_m\|^2+2(\mathbf{q}_{m,w}-\mathbf{L}^r_m)^\dagger(\mathbf{L}^r_m-\mathbf{L}_m). \tag{46}$$

Substituting $\|\mathbf{q}_{m,w}-\mathbf{L}_m\|^2$ by $V_{m,w}$, $\check{R}_{m,n}$ can be reformulated as

$$\check{R}^w_{m,n}\leq\log_2\left(\frac{\rho_0}{H_0^2+V_{m,w}}\sum_{j=1}^{n-1}P_{m,j}+\sigma^2\right)\triangleq\ddot{R}^w_{m,n}, \tag{47}$$

which is convex.

Finally, $R^w_{m,n}$ can be approximated to a concave function, which satisfies

$$R^w_{m,n}\tau_m\geq\left(\dot{R}^w_{m,n}-\ddot{R}^w_{m,n}\right)\tau_m\geq\delta_{m,n}. \tag{48}$$

From the above derivation, all the constraints have been transformed into convex ones. In addition, the sum throughput can be expressed as

$$R_{sum}=\sum_{m=1}^{M}\sum_{n=1}^{N_m}\min\{\dot{R}^1_{m,n}-\ddot{R}^1_{m,n},\cdots,\dot{R}^n_{m,n}-\ddot{R}^n_{m,n}\}\tau_m, \tag{49}$$

which is concave. Thus, the location optimization can be transformed as

$$\begin{aligned}(\mathrm{P3}):\max_{\mathbf{L},\mathrm{V_{m,w}}}\ & R_{sum}\\ s.t.\ & \left(\dot{R}^w_{m,n}-\ddot{R}^w_{m,n}\right)\tau_m\geq\delta_{m,n}, && \text{(50a)}\\ & \|\mathbf{q}_{m,w}-\mathbf{L}_m\|^2\leq\rho_0\frac{P_{m,n}-\eta_{m,n}\sum_{j=1}^{n-1}P_{m,j}}{\eta_{m,n}\sigma^2}-H_0^2, && \text{(50b)}\\ & \sum_{i=1}^{M}\|\mathbf{L}_{\mathbf{G}(i+1)}-\mathbf{L}_{\mathbf{G}(i)}\|\leq S_{min}, && \text{(50c)}\\ & V_{m,w}\geq 0, w\leq n\in\mathbf{\Gamma_m}, m\in\mathbf{\Lambda}, && \text{(50d)}\\ & V_{m,w}\leq\|\mathbf{q}_{m,w}-L^r_m\|^2+2(\mathbf{q}_{m,w}-\mathbf{L}^r_m)^\dagger(\mathbf{L}^r_m-\mathbf{L}_m), && \text{(50e)}\end{aligned}$$

which is convex and can be solved via CVX. Meanwhile, the decoding order should be updated according to the results.

D. Duration Optimization

The transmission duration $\mathbf{T}$ is optimized with $\mathbf{P}$ and $\mathbf{L}$ obtained by solving (P2) and (P3). Thus, we have

$$\begin{aligned}(\mathrm{P4}):\max_{\mathbf{T}}\ & \sum_{m=1}^{M}\sum_{n=1}^{N}R_{m,n}\tau_m\\ s.t.\ & \sum_{m=1}^{M}\tau_m\leq T_0-T_S, && \text{(51a)}\\ & R_{m,n}\tau_m\geq\delta_{m,n}, n\in\mathbf{\Gamma_m}, m\in\mathbf{\Lambda}. && \text{(51b)}\end{aligned}$$

To obtain the flying duration T_S, assume that the maximum speed of UAV is ν. During the flight, the UAV first accelerates to reach the maximum speed, then keeps the constant velocity motion, and finally decelerates to the next hovering location. Thus, the flying duration of UAV T_S can be calculated as

$$T_S=\frac{S_{min}-S_\alpha}{\nu}+T_\alpha, \tag{52}$$

where S_α and T_α are the sum distance and time during the accelerating and decelerating with the same acceleration α. Meanwhile, S_{min} can be updated in each iteration according to the optimized locations. Thus, S_α and T_α can be expressed as

$$\begin{cases}S_\alpha=2M\cdot\dfrac{\nu^2}{2\alpha},\\ T_\alpha=2M\cdot\dfrac{\nu}{\alpha}.\end{cases} \tag{53}$$

As a result, for (51a), we have

$$\sum_{m=1}^{M}\tau_m\leq T_0-\frac{S_{min}}{\nu}-\frac{M\cdot\nu}{\alpha}. \tag{54}$$

Thus, (P4) is a standard linear programming, which can be solved by CVX directly.

Algorithm 3 - Alternating Optimization Algorithm for (P1)

1: **Initialization**: The initial transmission duration of UAV in each cluster τ_m^0 is set to $(T_0 - T_S)/M$. The initial locations are initialized as the centroids of each cluster, $L_m^0 = \sum_{n=1}^{N_m} q_{m,n}/N_m$. The initial power is allocated to satisfy the requirements of users. Set the initial index of iterations as $k = 0$.
2: **Repeat**
3: Set the initial index of iterations as $r = 0$.
4: **Repeat**
5: Solve (P2), and obtain the optimal power P^{r+1}.
6: Solve (P3), and obtain the optimal location L^{r+1}.
7: Adjust the decoding order in each cluster via L^{r+1}.
8: Update: $r = r + 1$.
9: **Until P** and **L** are convergent.
10: Solve (P4), obtain the optimized duration T^{k+1}.
11: Update: $k = k + 1$.
12: **Until** convergence.
13: Output: **P**, **L**, **T** and the throughput.

E. Proposed Algorithm

Accordingly, the problem (P1) have been divided into three subproblems, which are transformed into convex ones. Thus, we propose an iterative algorithm to solve the problem, summarized as Algorithm 3, with its convergence proved as follows.

Assume that the throughput in the r-th inner iteration and the k-th outer iteration is $R_{sum}(P^r, L^r, T^k)$. By Step 5 and Step 6 in Algorithm 3, we can obtain better power allocation P^{r+1} and hovering location L^{r+1}, and have

$$R_{sum}(P^{r+1}, L^{r+1}, T^k) \geq R_{sum}(P^r, L^r, T^k). \tag{55}$$

In Step 7, the decoding order is updated, and the throughput cannot always decrease. After Step 10, the duration is re-allocated via P^r and L^r. The throughput cannot decrease. Thus, we have

$$R_{sum}(P^r, L^r, T^{k+1}) \geq R_{sum}(P^r, L^r, T^k). \tag{56}$$

Since the resource is limited, the throughput has a specific upper bound, and cannot always decrease. Therefore, Algorithm 3 is convergent.

In Algorithm 3, (P2) and (P3) are solved by SCA, the computational complexity of which is about the number of iterations and optimization variables [33]. Since there are K users in the network, both (P2) and (P3) have K variables. Meanwhile, (P4) is a linear programming, whose computational complexity can be denoted as $\mathcal{O}\left(M\left(K+1\right)^2\right)$. Thus, the overall computational complexity of Algorithm 3 can be calculated as

$$\mathcal{O}\left(I_2\left(2I_1K^3 + M\left(K+1\right)^2\right)\right), \tag{57}$$

where I_1 and I_2 represent the number of inner and outer iterations, respectively.

TABLE I
PERFORMANCE COMPARISON OF GA AND ES

	Z	β	S_{min} (km)	Complexity
ES with 7 clusters			3.3686	$\mathcal{O}$(5040)
GA with 7 clusters	30	50	3.5007	$\mathcal{O}$(73500)
ES with 8 clusters			3.9018	$\mathcal{O}$(40320)
GA with 8 clusters	40	50	4.0382	$\mathcal{O}$(128000)
ES with 9 clusters			3.9691	$\mathcal{O}$(362880)
GA with 9 clusters	40	50	4.2639	$\mathcal{O}$(162000)
ES with 10 clusters			4.2669	$\mathcal{O}$(3628800)
GA with 10 clusters	50	50	4.6848	$\mathcal{O}$(250000)
ES with 11 clusters			4.6234	$\mathcal{O}$(39916800)
GA with 11 clusters	50	50	4.9502	$\mathcal{O}$(302500)

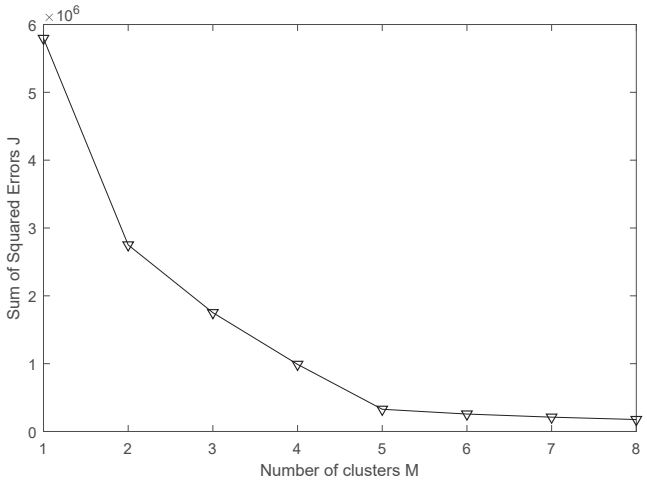

Fig. 2. The value of $\mathcal{J}$ with M increasing in the K-means algorithm when there are 19 users.

V. SIMULATION RESULTS AND DISCUSSION

In this section, simulation results are presented to demonstrate the effectiveness of the proposed scheme. The parameters are set as follows. The power of AWGN σ^2 is set as -110 dBm. In addition, we set the reference channel coefficient ρ_0 as -60 dB. Assume that all the users have the same QoS requirement and throughput threshold, i.e., $\eta_{m,n} = \eta_0, \delta_{m,n} = \delta_0 = 3$ bit/Hz, $n \in \mathbf{\Gamma_m}, m \in \mathbf{\Lambda}$. To establish LoS links, the altitude of UAV H_0 is set to 150 m. Meanwhile, the maximum speed and acceleration of UAV are set as $\nu = 8$ m/s and $\alpha = 4$ m/s^2, respectively.

To prove the effectiveness of Algorithm 2, the proposed GA algorithm is compared with ES in Table 1. In the simulation, the mutation probability ϱ is set to 0.4. Furthermore, to achieve better performance, the number of individuals Z needs to increase with M. Since the results obtained by GA are not fixed, the GA algorithm is performed 100 times, and the average results are shown. From the comparison, we can find that the computational complexity of GA is much less than that of ES when the number of clusters M is no smaller than 9. Furthermore, the results obtained by GA are very close to those by ES. Thus, we can adopt the ES when $M < 9$, otherwise, the GA-based algorithm is performed to optimize the UAV routing.

From Fig. 2 to Fig. 7, we first consider the NOMA-UAV network with 19 users, which can be divided into 5 clusters

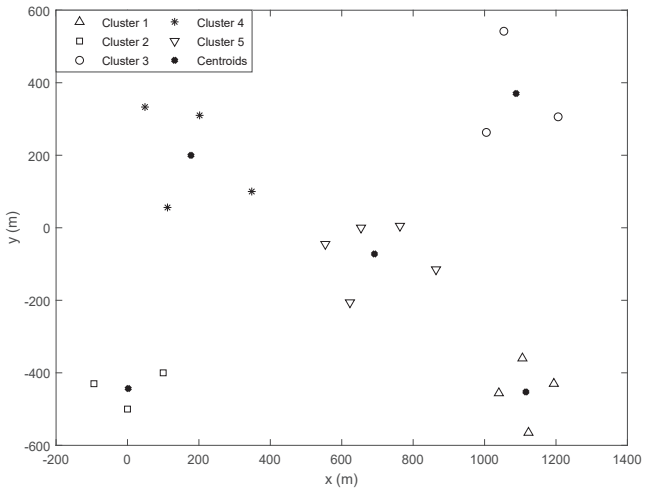

Fig. 3. User clustering results via the K-means algorithm with 19 users.

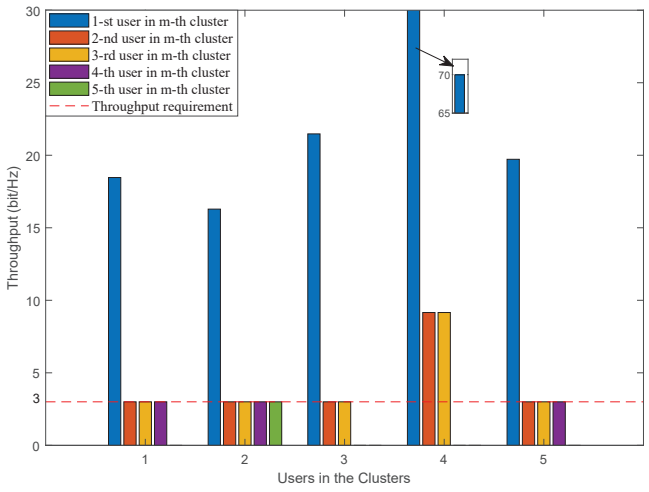

Fig. 5. Throughput of each user with $\eta_0 = 1.0$ when there are 19 users in the network.

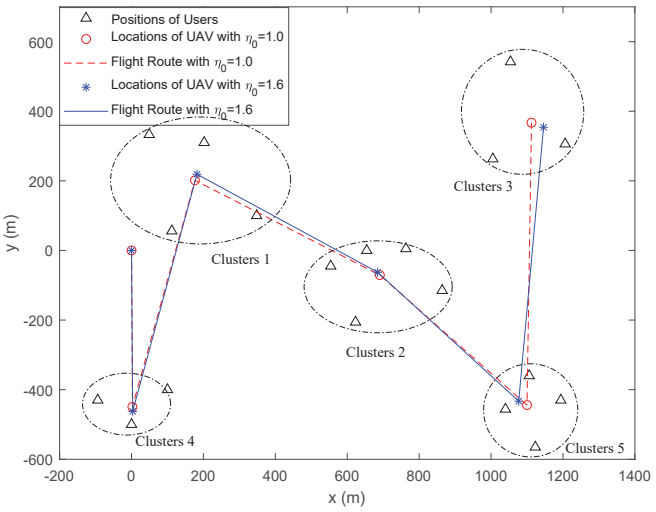

Fig. 4. Optimal routing and hovering locations of UAV with different QoS requirements.

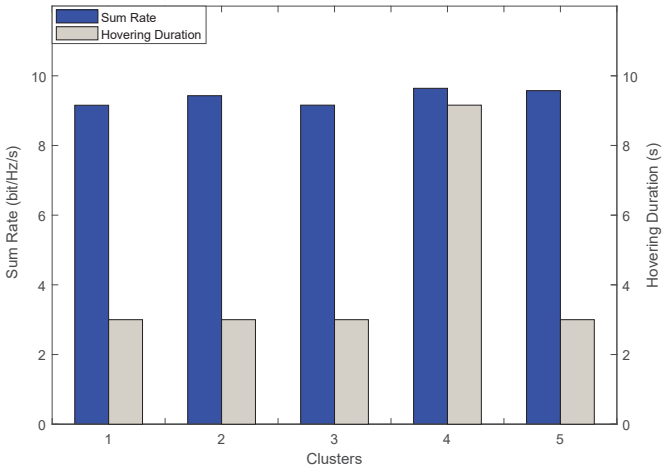

Fig. 6. Sum rate and hovering duration for the 5 clusters with $\eta_0 = 1.0$.

by Algorithm 1. To guarantee that the UAV can complete all the tasks, the whole duration T_0 is set as 415 s.

Fig. 2 and Fig. 3 show the clustering results of the K-means algorithm. The values of $\mathcal{J}$ with the increase of M are first shown in Fig. 2. From the results, we can find that the value of $\mathcal{J}$ sharply decreases before $M = 5$, after which the trend gets stable. According to the elbow method, the suitable number of clusters M is 5. The result of user clustering is presented in Fig. 3. From the results, we can see that the distributed randomly users can be effectively grouped into 5 clusters by the K-means algorithm.

Fig. 4 shows the optimal routing and hovering locations of UAV with different QoS requirements. Since the number of clusters is 5, we adopt ES to search the optimal routing. Meanwhile, the total transmission power P_{sum} of UAV is set as 0.2 W. From the results, we can see that the UAV routing and locations can be effectively optimized. Furthermore, we find that the optimal UAV locations get closer to the users with better channels when the QoS threshold of users η_0 increases. This is because the users with worse channels will be allocated more power to achieve higher QoS. Due to the limited power, the users with better channels will be allocated less. Therefore, the locations of UAV get closer to the users with better channels to compensate for their transmission power.

In Fig. 5 and Fig. 6, we set $\eta_0 = 1.0$. The throughput of each user is first shown in Fig. 5. We can find that the throughput requirement of each user can be satisfied by the proposed scheme. Furthermore, we show the sum rate and duration allocated for each cluster in Fig. 6. From the results in Fig. 5 and Fig. 6, we can find that the resource allocated to the users with worse channels can just satisfy their requirements, and more resource trends to be allocated to the user with the best channel in each cluster to maximize the sum throughput.

The sum throughput of the proposed scheme is compared with benchmarks in Fig. 7. The first benchmark is the OFDMA scheme, which can be solved by SCA. The second benchmark is the NOMA scheme, where the hovering locations are the centroids of clusters determined by the method in [25]. The results show that the proposed scheme has much better performance than both the two benchmarks. Furthermore, in

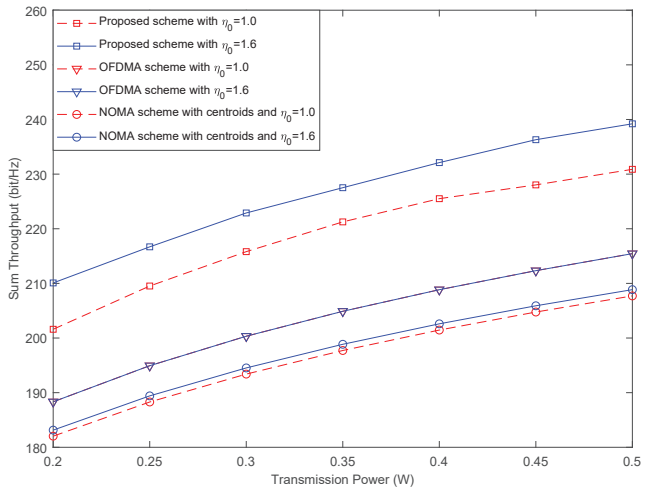

Fig. 7. Sum throughput of the proposed scheme and benchmarks with different the transmission power.

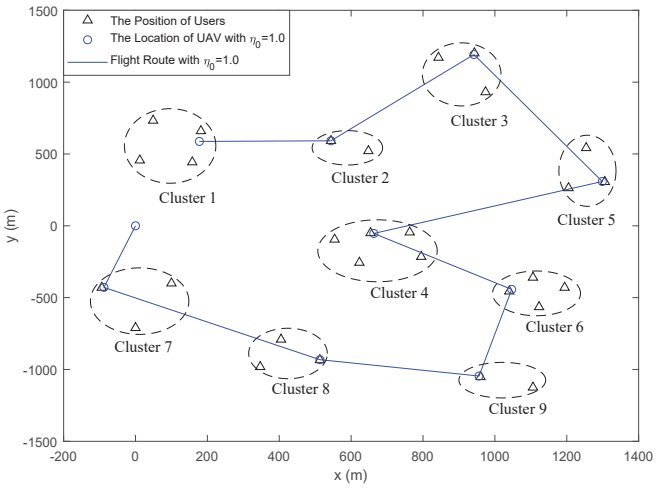

Fig. 8. The optimal locations and routing of UAV with $\eta_0 = 1.0$ for the case of 29 users in 9 clusters.

the two schemes with NOMA, the sum throughput is higher with stricter QoS requirement. This is because higher QoS means higher achievable rate, and less transmission duration is needed for the clusters with worse channels. In this way, more transmission duration can be allocated to the clusters with the better channels, and the sum throughput can be improved. On the other hand, the throughput of OFDMA is not affected by QoS requirements, because the transmission power is almost equally distributed among users. The SINR can reach a high level for each user, which exceed the QoS requirements.

After that, we consider the NOMA-UAV network of 29 users to verify the effectiveness of the proposed scheme with more users. We set the QoS threshold η_0 and T_0 to 1.0 and 489 s, respectively. The positions of users, optimized routing and hovering locations of UAV are shown in Fig. 8. In the network, the users are divided into 9 clusters by Algorithm 1. Accordingly, the optimal routing of UAV can be obtained by GA in Algorithm 2. From the results, we can find that the GA-based algorithm can effectively optimize the UAV routing. Then, we show the throughput of each user when there are 29

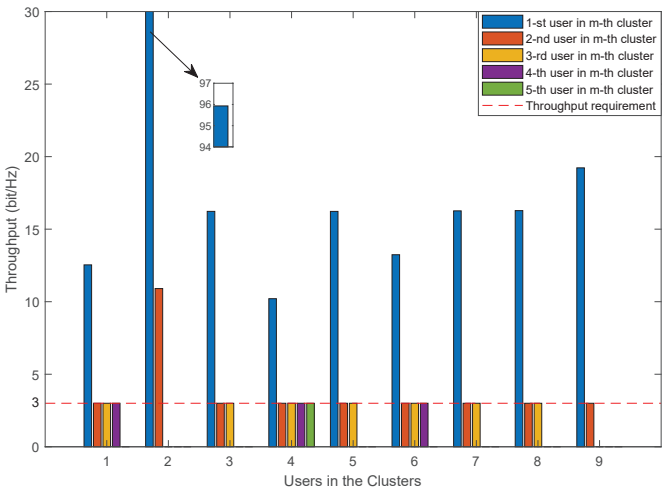

Fig. 9. Throughput of each user with $\eta_0 = 1.0$ when there are 29 users in the network.

users in Fig. 9. From the result, we can find that the proposed scheme can satisfy the throughput threshold of 3 bit/Hz for all the users, and the throughput of the 2nd cluster highly exceeds the threshold. This is because the 2nd cluster has the best channel condition, and more resource will be allocated to it to maximize the sum throughput.

VI. Conclusion

In this paper, we have proposed a resource allocation scheme to maximize the sum throughput of the NOMA-UAV network with multiple clusters. To satisfy the QoS requirements of all users, we first propose a K-means algorithm to group the users into M clusters. In addition, GA is adopted to obtain the optimal routing of UAV. Based on the optimal clusters and routing, we jointly optimize the transmission power, hovering locations and transmission duration of UAV to maximize the sum throughput, which is a non-convex problem. We divide it into three subproblems including two non-convex subproblems and a linear programming one. Thus, we adopt SCA to transform the non-convex subproblems into convex ones. Finally, an iterative algorithm is proposed to solve the resource allocation problem. Simulation results show that the proposed scheme is effective and has better performance than the benchmarks.

References

[1] Q. Huang, W. Wang, W. Lu, N. Zhao, A. Nallanathan, and X. Wang, "Throughput maximization for multi-cluster NOMA-UAV networks," in *Proc. IEEE GLOBECOM'22*, pp. 1–6, Rio de Janeiro, Brazil, Dec. 2022.
[2] Y. Zeng, R. Zhang, and T. J. Lim, "Wireless communications with unmanned aerial vehicles: opportunities and challenges," *IEEE Commun. Mag.*, vol. 54, no. 5, pp. 36–42, May, 2016.
[3] N. Zhao, W. Lu, M. Sheng, Y. Chen, J. Tang, F. R. Yu, and K.-K. Wong, "UAV-assisted emergency networks in disasters," *IEEE Wireless Commun.*, vol. 26, no. 1, pp. 45–51, Feb. 2019.
[4] A. A. Khuwaja, Y. Chen, N. Zhao, M.-S. Alouini, and P. Dobbins, "A survey of channel modeling for UAV communications," *IEEE Commun. Surveys Tuts.*, vol. 20, no. 4, pp. 2804–2821, 4th Quart. 2018.
[5] L. Gupta, R. Jain, and G. Vaszkun, "Survey of important issues in UAV communication networks," *IEEE Commun. Surveys Tuts.*, vol. 18, no. 2, pp. 1123–1152, 2nd Quart. 2016.

[6] X. Lin, V. Yajnanarayana, S. D. Muruganathan, S. Gao, H. Asplund, H.-L. Maattanen, M. Bergstrom, S. Euler, and Y.-P. E. Wang, "The sky is not the limit: LTE for unmanned aerial vehicles," *IEEE Commun. Mag.*, vol. 56, no. 4, pp. 204–210, Apr. 2018.

[7] Y. Zeng, Q. Wu, and R. Zhang, "Accessing from the sky: A tutorial on UAV communications for 5G and beyond," *Proc. IEEE*, vol. 107, no. 12, pp. 2327–2375, Dec. 2019.

[8] Y. Zeng, R. Zhang, and T. J. Lim, "Throughput maximization for UAV-enabled mobile relaying systems," *IEEE Trans. Commun.*, vol. 64, no. 12, pp. 4983–4996, Dec. 2016.

[9] Q. Wu, Y. Zeng, and R. Zhang, "Joint trajectory and communication design for multi-UAV enabled wireless networks," *IEEE Trans. Wireless Commun.*, vol. 17, no. 3, pp. 2109–2121, Mar. 2018.

[10] H. Wang, G. Ren, J. Chen, G. Ding, and Y. Yang, "Unmanned aerial vehicle-aided communications: Joint transmit power and trajectory optimization," *IEEE Wireless Commun. Lett.*, vol. 7, no. 4, pp. 522–525, Aug. 2018.

[11] Q. Wu and R. Zhang, "Common throughput maximization in UAV-enabled OFDMA systems with delay consideration," *IEEE Trans. Commun.*, vol. 66, no. 12, pp. 6614–6627, Dec. 2018.

[12] K. Meng, Q. Wu, S. Ma, W. Chen, and T. Q. S. Quek, "UAV trajectory and beamforming optimization for integrated periodic sensing and communication," *IEEE Wireless Commun. Lett.*, vol. 11, no. 6, pp. 1211–1215, Jun. 2022.

[13] Z. Ding, X. Lei, G. K. Karagiannidis, R. Schober, J. Yuan, and V. K. Bhargava, "A survey on non-orthogonal multiple access for 5G networks: Research challenges and future trends," *IEEE J. Select. Areas Commun.*, vol. 35, no. 10, pp. 2181–2195, Oct. 2017.

[14] S. M. R. Islam, N. Avazov, O. A. Dobre, and K.-s. Kwak, "Power-domain non-orthogonal multiple access (NOMA) in 5G systems: Potentials and challenges," *IEEE Commun. Surveys Tuts.*, vol. 19, no. 2, pp. 721–742, 2nd Quart. 2017.

[15] Y. Liu, S. Zhang, X. Mu, Z. Ding, R. Schober, N. Al-Dhahir, E. Hossain, and X. Shen, "Evolution of NOMA toward next generation multiple access (NGMA) for 6G," *IEEE J. Select. Areas Commun.*, vol. 40, no. 4, pp. 1037–1071, Apr. 2022.

[16] Z. Ding, P. Fan, G. K. Karagiannidis, R. Schober, and H. V. Poor, "NOMA assisted wireless caching: Strategies and performance analysis," *IEEE Trans. Commun.*, vol. 66, no. 10, pp. 4854–4876, Oct. 2018.

[17] Z. Chen, Z. Ding, X. Dai, and R. Zhang, "An optimization perspective of the superiority of NOMA compared to conventional OMA," *IEEE Trans. Signal Process.*, vol. 65, no. 19, pp. 5191–5202, Oct. 2017.

[18] C.-L. Wang, J.-Y. Chen, and Y.-J. Chen, "Power allocation for a downlink non-orthogonal multiple access system," *IEEE Wireless Commun. Lett.*, vol. 5, no. 5, pp. 532–535, Oct. 2016.

[19] Z. Yang, C. Pan, W. Xu, Y. Pan, M. Chen, and M. Elkashlan, "Power control for multi-cell networks with non-orthogonal multiple access," *IEEE Trans. Wireless Commun.*, vol. 17, no. 2, pp. 927–942, Feb. 2018.

[20] Z. Xiao, L. Zhu, J. Choi, P. Xia, and X.-G. Xia, "Joint power allocation and beamforming for non-orthogonal multiple access (NOMA) in 5G millimeter wave communications," *IEEE Trans. Wireless Commun.*, vol. 17, no. 5, pp. 2961–2974, May 2018.

[21] L. Zhu, J. Zhang, Z. Xiao, X. Cao, D. O. Wu, and X.-G. Xia, "Joint power control and beamforming for uplink non-orthogonal multiple access in 5G millimeter-wave communications," *IEEE Trans. Wireless Commun.*, vol. 17, no. 9, pp. 6177–6189, Sept. 2018.

[22] S. Feng, T. Bai, and L. Hanzo, "Joint power allocation for the multi-user NOMA-downlink in a power-line-fed VLC network," *IEEE Trans. Veh. Technol.*, vol. 68, no. 5, pp. 5185–5190, May 2019.

[23] N. Zhao, X. Pang, Z. Li, Y. Chen, F. Li, Z. Ding, and M.-S. Alouini, "Joint trajectory and precoding optimization for UAV-assisted NOMA networks," *IEEE Trans. Commun.*, vol. 67, no. 5, pp. 3723–3735, May 2019.

[24] Y. Liu, Z. Qin, Y. Cai, Y. Gao, G. Y. Li, and A. Nallanathan, "UAV communications based on non-orthogonal multiple access," *IEEE Wireless Commun.*, vol. 26, no. 1, pp. 52–57, Feb. 2019.

[25] X. Liu, J. Wang, N. Zhao, Y. Chen, S. Zhang, Z. Ding, and F. R. Yu, "Placement and power allocation for NOMA-UAV networks," *IEEE Wireless Commun. Lett.*, vol. 8, no. 3, pp. 965–968, Jun. 2019.

[26] R. Zhang, X. Pang, J. Tang, Y. Chen, N. Zhao, and X. Wang, "Joint location and transmit power optimization for NOMA-UAV networks via updating decoding order," *IEEE Wireless Commun. Lett.*, vol. 10, no. 1, pp. 136–140, Jan. 2021.

[27] W. Feng, N. Zhao, S. Ao, J. Tang, X. Zhang, Y. Fu, D. K. C. So, and K.-K. Wong, "Joint 3D trajectory and power optimization for UAV-aided mmwave MIMO-NOMA networks," *IEEE Trans. Commun.*, vol. 69, no. 4, pp. 2346–2358, Apr. 2021.

[28] M. Katwe, K. Singh, P. K. Sharma, C.-P. Li, and Z. Ding, "Dynamic user clustering and optimal power allocation in UAV-assisted full-duplex hybrid NOMA system," *IEEE Trans. Wireless Commun.*, vol. 21, no. 4, pp. 2573–2590, Apr. 2022.

[29] C. Pan, H. Ren, Y. Deng, M. Elkashlan, and A. Nallanathan, "Joint blocklength and location optimization for URLLC-enabled UAV relay systems," *IEEE Commun. Lett.*, vol. 23, no. 3, pp. 498–501, Jan. 2019.

[30] J. Cui, Z. Ding, P. Fan, and N. Al-Dhahir, "Unsupervised machine learning-based user clustering in millimeter-wave-NOMA systems," *IEEE Trans. Wireless Commun.*, vol. 17, no. 11, pp. 7425–7440, Mar. 2019.

[31] R. Tibshirani, G. Walther, and T. Hastie, "Estimating the number of clusters in a data set via the gap statistic," *Statist. Methodol.*, vol. 63, no. 2, pp. 411–423, Jan. 2002.

[32] T. Li and Z. Ge, "A multiple QoS anycast routing algorithm based adaptive genetic algorithm," *Proc. 3d Int. Conf. Genetic Evol. Comput.*, pp. 89–92, Oct. 2009.

[33] C. Zhan and Y. Zeng, "Aerialground cost tradeoff for multi-UAV-enabled data collection in wireless sensor networks," *IEEE Trans. Commun.*, vol. 68, no. 3, pp. 1937–1950, Mar. 2020.

Resource Allocation for Multi-Cluster NOMA-UAV Networks

Qiulei Huang*, Wei Wang*, Weidang Lu†, *Senior Member, IEEE*, Nan Zhao*, *Senior Member, IEEE*, Arumugam Nallanathan‡, *Fellow, IEEE*, and Xianbin Wang§, *Fellow, IEEE*

*Dalian University of Technology, Dalian, China

†Zhejiang University of Technology, Hangzhou, China

‡Queen Mary University of London, London, U.K.

§Western University, London, Canada

Abstract

Combining non-orthogonal multiple access (NOMA) and unmanned aerial vehicles (UAVs) could achieve better performance for wireless networks. However, effective resource allocation for quality of service (QoS) provision among all users still remains as a great challenge for multi-cluster NOMA-UAV networks. In this paper, we propose a NOMA-UAV scheme, where a UAV is deployed as the mobile base station to serve ground users. To meet the QoS requirements of all users with limited resource, the user clustering and optimal routing are first developed by the K-means algorithm and genetic algorithm, respectively. Then, the sum throughput is maximized by jointly optimizing the transmission power, hovering locations and transmission duration of UAV. To solve this non-convex problem with coupled variables, we decompose it into three subproblems. Among them, the power and location optimizations are also non-convex, which can be transformed into convex ones by successive convex approximation. The duration optimization is a linear programming which can be solved directly. Then, we propose an iterative algorithm to solve these three subproblems alternately. Finally, simulation results are presented to show the effectiveness of the proposed scheme.

Index Terms

Genetic algorithm, K-means, non-orthogonal multiple access, resource allocation, unmanned aerial vehicle.

Part of this paper will be presented at IEEE GLOBECOM 2022 [1].

I. Introduction

Recently, unmanned aerial vehicle (UAV) assisted wireless communication has become an important supplement to the terrestrial networks. On one hand, UAVs can be deployed flexibly due to the mobility [2], and thus, UAV-assisted communication is an effective solution for emergency communications without infrastructure [3]. On the other hand, the UAV-to-ground channels can be approximated as the high-quality line-of-sight (LoS) links [4]. Owing to these advantages, UAV-assisted communications have attracted great attentions from both academia and industry [5]–[7]. In [5], Gupta *et al.* identified the main challenges for UAV-assisted wireless networks. The channel models of UAV-aided communications were studied by Lin *et al.* in [6]. In [7], Zeng *et al.* introduced how to integrate UAVs into the fifth-generation and future wireless networks. However, the operation life of UAV is limited, due to the finite onboard energy. For this reason, how to allocate the resource effectively still remains a great challenge for UAV-assisted communications [8]–[11]. In [8], Zeng *et al.* deployed UAVs as the relaying nodes to maximize the system throughput by iteratively optimizing the power allocation and UAV trajectory. The minimum throughput of all ground users was maximized by Wu *et al.* via jointly adjusting the multi-user scheduling and UAV trajectory in [9]. In [10], Wang *et al.* proposed an effective algorithm to improve the throughput by jointly optimizing the transmission power and trajectory. In [11], the UAV trajectory and resource allocation were optimized by Wu and Zhang to maximize the minimum average throughput. In [12], Meng *et al.* jointly adjusted the UAV trajectory, transmit precoder and sensing start instant to maximize the achievable rate in UAV-enabled integrated sensing and communication systems.

On the other hand, non-orthogonal multiple access (NOMA) is becoming a promising technology to satisfy the requirements of super-high rate, ultra-low latency, ultra-reliability and

massive connectivity [13]. In the power-domain NOMA, more power will be allocated to the users with worse channels to allow them to share the same resource block [14]. Then, the high-power signals are first decoded and removed via successive interference cancellation (SIC) before decoding the lower ones. In [15], Liu *et al.* presented the current research efforts and future application scenarios for NOMA. Ding *et al.* proposed two NOMA-assisted caching strategies to provide additional bandwidth in [16]. In [17], Chen *et al.* proved that NOMA can always achieve better performance than orthogonal multiple access (OMA) when both have the optimal resource allocation policies. However, there exists serious interference between users because they share the same resource block. Thus, the power allocation is extremely significant for NOMA systems [18]–[22]. In [18], Wang *et al*. proposed a power allocation scheme to maximize the sum capacity for single-input single-output NOMA system with two users. Yang *et al.* adopted power control for multi-cell downlink NOMA networks to minimize the sum power while maximizing the sum rate in [19]. In [20], Xiao *et al.* maximized the sum rate for millimeter-wave NOMA communications by jointly optimizing the transmission power and beamforming. The transmission rate was maximized by Zhu *et al.* through jointly optimizing the transmission power and beamforming for uplink NOMA in [21]. In [22], Feng *et al.* designed a power allocation algorithm, which adopts NOMA to maximize the sum throughput.

Due to their own advantages, it is natural to integrate NOMA into UAV-assisted communications to further improve the performance [23]–[26]. Zhao *et al.* proposed an effective algorithm in [23] to maximize the sum rate via jointly adjusting the trajectory and NOMA precoding. In [24], Liu *et al.* proposed a unified framework to study the UAV-aided networks with massive access capability supported by NOMA. In [25], the sum rate was maximized by Liu *et al.* through jointly optimizing the location of UAV and the transmission power for NOMA-UAV

networks. Furthermore, the decoding order was considered by Zhang *et al.* in [26] to achieve better performance than the scheme in [25].

When there are more users to be served by the UAV, only a single NOMA group cannot accommodate all of them, and we should divide them into multiple clusters. Accordingly, NOMA can be utilized in each cluster. However, to the best of our knowledge, the resource allocation design for NOMA-UAV networks with multiple clusters has not been fully investigated, and only a few literatures have focused on this direction [27], [28]. In [27], the sum rate was maximized by Feng *et al.* through jointly adjusting the three-dimensional locations of UAV, beam pattern and transmission power, where the optimal UAV routing was obtained by the branch and bound algorithm. In [28], Katwe *et al.* deployed multiple UAVs to improve the sum rate of the NOMA-UAV system by dynamic user clustering, optimal UAV placement and power allocation, where each cluster was served by a single UAV.

Inspired by the above-mentioned works, in this paper, we propose a resource allocation scheme to maximize the sum throughput for multi-cluster NOMA-UAV networks. Different from [27] and [28], the users are first clustered by the K-means algorithm. To reduce the computational complexity, the UAV routing is obtained by the genetic algorithm. In addition, the decoding order and global impact are also considered to improve the performance when optimizing the transmission power, hovering locations and transmission duration. In summary, the main motivations and contributions of this paper are as follows:

- A new effective multi-cluster scheme for NOMA-UAV networks is proposed to satisfy the quality of service (QoS) of all the users with limited resource. The sum throughput of the network is maximized by optimizing the user clustering, UAV routing and hovering locations, SIC decoding order, transmission power as well as duration allocation.

- A NOMA clustering algorithm is first developed by the K-means algorithm to support the proposed multi-cluster scheme, which are closely related to the distribution of user positions. Accordingly, the UAV routing optimization with multiple clusters can be deemed as a traveling salesman problem (TSP), and we propose a GA-based algorithm to solve it, which can greatly decrease the computational complexity.
- Based on the optimized user clustering and UAV routing, the sum throughput maximization problem is decomposed into three subproblems of transmission power, hovering locations and transmission duration, which can be transformed into convex ones by successive convex approximation (SCA). Then, we propose an iterative algorithm to solve these subproblems alternately.

The rest of this paper is organized as follows. In Section II, the system model is presented. User clustering and UAV routing are optimized in Section III. In Section IV, the sum throughput is maximized by jointly optimizing the locations, power and duration. Simulation results and discussion are shown in Section V, followed by the conclusion in Section VI.

Notation: $\|\mathbf{L}\|$ and $\mathbf{L}^{\dagger}$ denote the Euclidean norm and transpose matrix of $\mathbf{L}$. $\mathbb{R}^{2\times 1}$ is the space of 2×1 matrices. $\bigtriangledown f(x)$ represents the gradient function of $f(x)$. The factorial of M is denoted as $M!$.

II. System Model

Consider a NOMA-UAV network where a UAV is deployed as the mobile base station (BS) with a single antenna to serve K single-antenna ground users as shown in Fig. 1. The users are assumed to be divided into M clusters. Define the set of clusters as $\mathbf{\Lambda} = \{1, 2, ..., M\}$. There are N_m users in the m-th cluster. The set of users in the m-th cluster is defined as

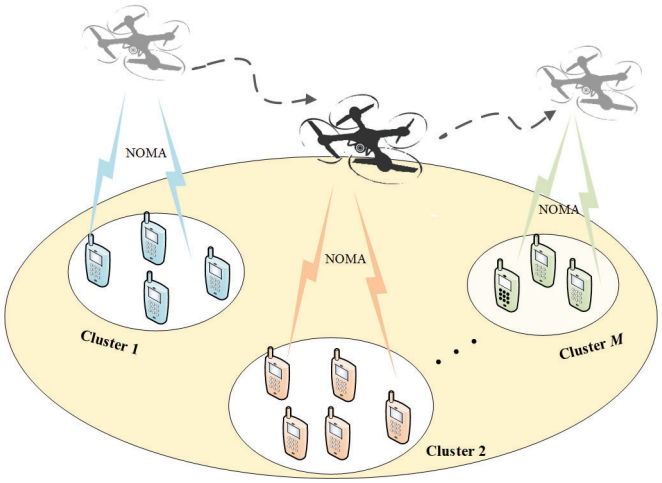

Fig. 1. A K-user NOMA-UAV network with M clusters.

$\mathbf{\Gamma_m} = \{1, 2, ..., N_m\}, m \in \mathbf{\Lambda}$. Thus, we have

$$K = \sum_{m=1}^{M} N_m, m \in \mathbf{\Lambda}. \tag{1}$$

The UAV takes off from the initial point, and sequentially flies to the hovering point of each cluster according to the predefined trajectory. The transmission is performed only when hovering to avoid the Doppler effect. Meanwhile, to achieve high spectrum efficiency and massive connections, the UAV serves the users in each cluster via NOMA.

The whole duration T_0 can be divided into the flying duration T_S and the transmission duration. The transmission duration for the m-th cluster is denoted as τ_m. Thus, we have

$$\sum_{m=1}^{M} \tau_m + T_S \leq T_0. \tag{2}$$

Denote the n-th user in the m-th cluster as $U_{m,n}$. The distance from the UAV to $U_{m,n}$ when connected can be represented by $d_{m,n}$. Assume that the UAV is flying at the altitude H_0. Define the horizontal hovering coordinate of the UAV for the m-th cluster as $\mathbf{L}_m = [A_m, B_m]^\dagger \in \mathbb{R}^{2\times 1}$, and the position of $U_{m,n}$ as $\mathbf{q}_{m,n} = [a_{m,n}, b_{m,n}]^\dagger \in \mathbb{R}^{2\times 1}$. Therefore, $d_{m,n}$ can be calculated as

$$d_{m,n} = \sqrt{H_0^2 + \parallel \mathbf{q}_{m,n} - \mathbf{L}_m \parallel^2}, n \in \mathbf{\Gamma_m}, m \in \mathbf{\Lambda}. \tag{3}$$

Without loss of generality, in the m-th cluster, we assume

$$d_{m,1} \leq d_{m,2} \leq \cdots \leq d_{m,N_m}. \tag{4}$$

Define $h_{m,n}$ as the channel coefficient from the UAV to $U_{m,n}$. According to [29], the LoS probability is almost 1 when the UAV is higher than a suitable altitude, e.g., 120 m. Thus, the air-ground channels can be approximated as LoS, which is expressed as

$$\mid h_{m,n} \mid^2 = \rho_0 d_{m,n}^{-2}, \tag{5}$$

where ρ_0 is the reference channel coefficient of the unit distance 1 m.

According to NOMA, SIC is adopted at the receivers to guarantee the fairness among users, and the user with weaker channel will be compensated for more transmission power. Define $P_{m,n}$ as the transmission power for $U_{m,n}$. Thus, according to the distance order in (4), $P_{m,n}$ should satisfy

$$0 < P_{m,1} \leq P_{m,2} \leq ... \leq P_{m,N_m}. \tag{6}$$

Meanwhile, the sum transmission power for all the users in each cluster should not exceed the power limit of UAV P_{sum}, and we have

$$\sum_{n=1}^{N_m} P_{m,n} \leq P_{sum}. \tag{7}$$

Therefore, the received signal at $U_{m,i}$ can be expressed as

$$y_{m,i} = h_{m,i} \sum_{j=1}^{N_m} \sqrt{P_{m,j}} x_{m,j} + n_{m,i}, \tag{8}$$

where $n_{m,i}$ represents the additive white Gaussian noise (AWGN) with variance σ^2 and zero mean at $U_{m,i}$, and $x_{m,i}$ denotes the message of $U_{m,i}$ with the unit power of $|x_{m,i}|^2 = 1$.

In NOMA, each user first decodes the stronger signals and removes them from the superposed signal before decoding its own. Thus, according to (4), the signal-to-interference-plus-noise ratio

(SINR) for $U_{m,n}$ can be denoted as

$$\mathrm{SINR}_{m,n}=\frac{|h_{m,n}|^2 P_{m,n}}{|h_{m,n}|^2 \sum_{j=1}^{n-1} P_{m,j}+\sigma^2}, 2 \leq n \leq N_m. \tag{9}$$

In particular, when $n=1$, the SINR can be denoted as

$$\mathrm{SINR}_{m,1}=\frac{|h_{m,1}|^2 P_{m,1}}{\sigma^2}. \tag{10}$$

In addition, the messages from weaker users should be also correctly decoded at the receiver with better channel. Thus, we have the constraint as

$$\mathrm{SINR}_{m,n}^{min}=\min\{\mathrm{SINR}_{m,n}^{1}, \cdots, \mathrm{SINR}_{m,n}^{n}\} \geq \eta_{m,n}, \tag{11}$$

where $\eta_{m,n}$ is the QoS requirement of $U_{m,n}$. Define $\mathrm{SINR}_{m,n}^{w}, \{w \leq n \in \boldsymbol{\Gamma_m}\}$ as the SINR when the signal of $U_{m,n}$ is decoded at the receiver $U_{m,w}$, which can be expressed as

$$\mathrm{SINR}_{m,n}^{w}=\frac{|h_{m,w}|^2 P_{m,n}}{|h_{m,w}|^2 \sum_{j=1}^{n-1} P_{m,j}+\sigma^2}, w \leq n. \tag{12}$$

In particular, $\mathrm{SINR}_{m,n}^{w}=\mathrm{SINR}_{m,n}$ when $w=n$.

Accordingly, the downlink achievable rate of $U_{m,n}$ can be denoted as

$$R_{m,n}=\log_2(1+\mathrm{SINR}_{m,n}^{min}). \tag{13}$$

III. Clustering and Routing Optimization

As the available resource of UAV is limited, the user clustering and UAV flying route should be scheduled properly. To this end, we first utilize the K-means algorithm for user clustering in this section, and then propose a GA-based algorithm to optimize the UAV routing.

Algorithm 1 - K-means Algorithm for user clustering

1: **Initialization**: Randomly select M users as the initial centroids.
2: **Repeat**
3: For each user, calculate the Euclidean distance from it to each centroid.
4: Each user can be assigned to the cluster with the shortest distance from it.
5: Update the centroids by (14).
6: **Until** the centroids no longer change.
7: Output: $\boldsymbol{\Gamma_m}, \forall m \in \Lambda$.

A. User Clustering Optimization

In the network, the ground users locate in the distribution of clusters. Thus, the K-means algorithm can be adopted to realize the user clustering, which is an effective method with fast convergence. The specific algorithm is described as follows.

At first, we select M initial centroids randomly, with the centroid of the m-th cluster defined as $\boldsymbol{\mu}_m$. Calculate the distances from the users to each centroid. Each user is organized into the cluster whose centroid is closest to it. After all the users have been assigned, $\boldsymbol{\mu}_m$ can be updated as

$$\boldsymbol{\mu}_m = \frac{1}{N_m} \sum_{n=1}^{N_m} \mathbf{q}_{m,n}. \tag{14}$$

Then, the users are organized again according to the new centroids. The above steps are iteratively carried out until convergence [30]. The details of the proposed K-means algorithm are described in Algorithm 1.

To further improve the performance, choosing a proper M is important for the K-means algorithm. Thus, we introduce the sum of the squared errors as

$$\mathcal{J} = \sum_{m=1}^{M} \sum_{n=1}^{N_m} \|\mathbf{q}_{m,n} - \boldsymbol{\mu}_m\|^2, \tag{15}$$

which always decreases with the increase of M. A smaller value of $\mathcal{J}$ means that the result

of clustering is better. However, the clustering becomes ineffective when M gets close to K. Thus, we adopt the elbow method to obtain the proper M [31], in which the K-means algorithm is performed with different M. $\mathcal{J}$ decreases sharply before the elbow when M increases, after which the trend becomes stable. We can set this elbow as the proper value of M, which will be further demonstrated in Section V.

B. Routing Optimization

After the clusters are determined, we should find the optimal routing, which reflects the shortest flying distance for the UAV. The routing optimization can be deemed as a TSP. Generally, the optimal routing with M clusters can be obtained by the exhaustive search (ES), the computational complexity of which is $\mathcal{O}(M!)$. However, the complexity of ES becomes extremely high when the number of clusters increases. Thus, we propose a GA-based routing optimization algorithm, which can be described as follows.

1) *Encoding*: Assume that there are Z individuals in the t-th iteration, the set of which is defined as $\Omega^t = \{1, 2, \cdots, Z\}$. Each individual represents a UAV routing, which can be encoded as an array including the initial point and the cluster numbers from 1 to M. The index number of the initial point is set as 0, which locates at $\mathbf{L}_0 = (0, 0)$. We define the array $\mathbf{G}_z^t$ as the z-th individual in the t-th iteration. Thus, its distance $\lambda^t(z)$ can be calculated by

$$\lambda^t(z) = \sum_{i=1}^{M} \parallel \mathbf{L}_{\mathbf{G}_z^t(i+1)} - \mathbf{L}_{\mathbf{G}_z^t(i)} \parallel, z \in \Omega^t. \tag{16}$$

2) *Fitness Function*: The fitness function is crucial for the GA algorithm to evaluate the routes. Thus, the fitness function can be expressed as

$$\psi^t(z) = \frac{\lambda_{max}^t - \lambda^t(z) + \varepsilon_1}{\lambda_{max}^t - \lambda_{min}^t + \varepsilon_1}, \tag{17}$$

Algorithm 2 - GA for Routing Optimization

1: **Initialization**: Define the centroids of clusters as the initial hovering locations of UAV. Set the initial index of iterations as $t = 1$. Generate the initial generation with Z individuals.
2: **Repeat**
3: Calculate the fitness function $\psi^t(z)$ for each individual.
4: Find the individual with the largest fitness and decode the corresponding distance λ_{min}^t and route.
5: When $\lambda_{min}^t < S_{min}$, update $S_{min} = \lambda_{min}^t$ and **G** is the array of this individual.
6: **Repeat**
7: Generate ε_2 to select two ancestors.
8: Create the new route for the $(t+1)$-th iteration.
9: Generate ε_3.
10: Exchange the order of the two codes in this individual when $\varepsilon_3 \leq \varrho$.
11: **Until** the new routes are enough.
12: Update: $t = t + 1$.
13: **Until** $t = \beta$.
14: **Output**: **G** and S_{min}.

where λ_{max}^t and λ_{min}^t are the maximum and minimum distance in the t-th iteration, respectively. Meanwhile, we introduce a constant ε_1 to guarantee that the denominator of (17) is not equal to 0. Larger value of this function means that the corresponding route is better.

3) *Ancestor Selecting*: To generate the new routes for the next iteration, we need to select the individuals in the current iteration as ancestors via the roulette wheel selection. First, the cumulative probability of the z-th individual in the t-th iteration can be calculated as

$$\varphi^t(z) = \sum_{i=1}^{z} \frac{\psi^t(i)}{\sum_{j=1}^{Z} \psi^t(j)}, z \in \Omega^t. \tag{18}$$

Then, a random $\varepsilon_2 \in (0, 1]$ is generated. The z-th individual is selected as the ancestor when $\varphi^t(z-1) < \varepsilon_2 \leq \varphi^t(z)$. Repeat the operations until enough ancestors can be generated.

4) *Creating New Routes*: When creating the new routes, mutation is needed to avoid local optimums. Define ϱ as the mutation probability. The specific steps are as follows. First, a part of elements in an ancestor array is selected as the corresponding elements of the new route. Meanwhile, organize the rest elements of this route array according to the order of another ancestor's elements. Then, generate a random $\varepsilon_3 \in (0, 1)$. When $\varepsilon_3 \leq \varrho$, randomly exchange the order of the two elements in the new route.

Define the maximum number of iterations as β. Assume that the optimal routing is stored in a $(M+1)\times 1$ matrix $\mathbf{G}$. The shortest distance is denoted by S_{min}, which can be calculated by (16). The specific steps of GA are shown in Algorithm 2. The computational complexity of GA can be calculated by $\mathcal{O}(Z\beta M^2)$, which is dominated by creating the new routes [32]. Compared with the ES, the proposed GA-based algorithm can greatly decrease the computational complexity with the increasing number of clusters.

IV. Optimization for Maximizing Throughput

In this section, the resource of UAV is allocated based on the user clustering and routing optimization in Section III. We first formulate the problem of resource allocation, which is non-convex. Then, we decompose it into three subproblems. In the end, an effective algorithm is proposed to solve the subproblems alternately.

A. Problem Formulation

To take the full advantage of the resource, we aim at maximizing the system throughput by jointly optimizing the transmission power $\mathbf{P} = \{P_{m,n} | n \in \mathbf{\Gamma_m}, m \in \mathbf{\Lambda}\}$, the UAV hovering locations $\mathbf{L} = \{\mathbf{L}_m | m \in \mathbf{\Lambda}\}$ and the transmission duration allocation $\mathbf{T} = \{\tau_m | m \in \mathbf{\Lambda}\}$. Thus,

the optimization problem can be formulated as

$$
\begin{aligned}
(\mathrm{P1}): \max_{\mathbf{P},\mathbf{L},\mathbf{T}} & \sum_{m=1}^{M}\sum_{n=1}^{N_m} R_{m,n}\tau_m \\
s.t. & \sum_{m=1}^{M}\tau_m + T_S \leq T_0, && \text{(19a)} \\
& R_{m,n}\tau_m \geq \delta_{m,n}, && \text{(19b)} \\
& \mathrm{SINR}_{m,n}^{min} \geq \eta_{m,n}, n \in \boldsymbol{\Gamma_m}, m \in \boldsymbol{\Lambda}, && \text{(19c)} \\
& 0 < P_{m,1} \leq P_{m,2} \leq ... \leq P_{m,N_m}, && \text{(19d)} \\
& \sum_{n=1}^{N_m} P_{m,n} \leq P_{sum}, && \text{(19e)} \\
& \sum_{i=1}^{M} \|\mathbf{L}_{\mathbf{G}(i+1)} - \mathbf{L}_{\mathbf{G}(i)}\| \leq S_{min}. && \text{(19f)}
\end{aligned}
$$

In $(\mathrm{P1})$, (19a) defines the whole duration of UAV, including the flying and transmission duration. (19b) ensures that the throughput for $U_{m,n}$ should exceed a threshold $\delta_{m,n}$. The QoS of each user is guaranteed by (19c). (19d) restricts the power allocation according to the distance order in (4). The sum transmission power is limited by (19e). (19f) ensures that the flying distance cannot ascend with the change of hovering locations.

$(\mathrm{P1})$ is a non-convex problem with $\mathbf{P}, \mathbf{L}$ and $\mathbf{T}$ coupled, which is difficult to solve directly. To simplify $(\mathrm{P1})$, we decompose it into three subproblems, i.e., the transmit power optimization, the hovering location optimization and the duration optimization. Among them, both the power and location optimization are non-convex, which can be transformed into convex ones via the first order Taylor approximation. The duration optimization is a linear programming, which can be solved directly. In the end, we propose an effective algorithm to solve these three subproblems iteratively.

B. Transmission Power Optimization

For any given UAV location $\mathbf{L}$ and transmission duration $\mathbf{T}$, (P1) can be decomposed as

$$\max_{\mathbf{P}} \sum_{m=1}^{M}\sum_{n=1}^{N_m} R_{m,n}\tau_m$$

$$s.t.\ R_{m,n}\tau_m \geq \delta_{m,n}, \tag{20a}$$

$$\mathrm{SINR}_{m,n}^{min} \geq \eta_{m,n}, \tag{20b}$$

$$0 < P_{m,1} \leq P_{m,2} \leq ... \leq P_{m,N_m}, \tag{20c}$$

$$\sum_{n=1}^{N_m} P_{m,n} \leq P_{sum}, n \in \boldsymbol{\Gamma_m}, m \in \boldsymbol{\Lambda}, \tag{20d}$$

which is intractable due to the non-convex objective function and the constraints (20a) and (20b). Thus, SCA is adopted to approximate them as convex ones.

For the objective function and the constraints (20a), we have

$$\begin{aligned} R_{m,n} &= \log_2\left(1+\mathrm{SINR}_{m,n}^{min}\right) \\ &= \log_2\left(1+\min\{\mathrm{SINR}_{m,n}^{w}\}\right), w \leq n \in \boldsymbol{\Gamma_m}, \end{aligned} \tag{21}$$

where $\mathrm{SINR}_{m,n}^{min}$ can be obtained by Proposition 1.

Proposition 1: $\mathrm{SINR}_{m,n}^{min} = \mathrm{SINR}_{m,n}$.

Proof: $\mathrm{SINR}_{m,n}^{min} = \min\{\mathrm{SINR}_{m,n}^{w}\}$, and $\mathrm{SINR}_{m,n}^{w}$ can be rewritten as

$$\begin{aligned} \mathrm{SINR}_{m,n}^{w} &= \frac{|h_{m,w}|^2 P_{m,n}}{|h_{m,w}|^2 \sum_{j=1}^{n-1} P_{m,j} + \sigma^2} \\ &= \frac{P_{m,n}}{\sum_{j=1}^{n-1} P_{m,j} + \frac{\sigma^2}{|h_{m,w}|^2}}, \end{aligned} \tag{22}$$

We can find that $\mathrm{SINR}_{m,n}^{w}$ increases with $|h_{m,w}|^2$, which is determined by the distance $d_{m,n}$. To be specific, the users with longer distance always have the worse channels. Thus, the users with

larger index numbers have worse channels in each cluster according to the distance order in (4). Due to $w \leq n$, we can obtain $\mathrm{SINR}_{m,n}^{min} = \mathrm{SINR}_{m,n}^{n} = \mathrm{SINR}_{m,n}$. ■

Substituting $\mathrm{SINR}_{m,n}^{min}$ by $\mathrm{SINR}_{m,n}$ in $R_{m,n}$, we can obtain

$$\begin{aligned} R_{m,n} =& \log_2\left(1+\frac{|h_{m,n}|^2 P_{m,n}}{|h_{m,n}|^2\sum_{j=1}^{n-1}P_{m,j}+\sigma^2}\right) \\ =& \log_2\left(\frac{|h_{m,n}|^2\sum_{j=1}^{n}P_{m,j}+\sigma^2}{|h_{m,n}|^2\sum_{j=1}^{n-1}P_{m,j}+\sigma^2}\right), 2\leq n\leq N_m, \end{aligned} \tag{23}$$

which can be expanded as

$$\begin{aligned} R_{m,n} =& \log_2\left(|h_{m,n}|^2\sum_{j=1}^{n}P_{m,j}+\sigma^2\right) \\ & -\log_2\left(|h_{m,n}|^2\sum_{j=1}^{n-1}P_{m,j}+\sigma^2\right). \\ =& \widetilde{R}_{m,n}-\overline{R}_{m,n}. \end{aligned} \tag{24}$$

$R_{m,n}$ is a non-concave function with respect to $\mathbf{P}$ due to $\overline{R}_{m,n}$. Thus, we adopt the first-order Taylor expansion to approximate it.

Define $P_{m,n}^r$ as the transmission power of $U_{m,n}$ in the r-th iteration. Since $\overline{R}_{m,n}$ is concave, the first-order Taylor expansion of it at $P_{m,n}^r$ can be deduced as

$$\begin{aligned} \overline{R}_{m,n} =& \log_2\left(|h_{m,n}|^2\sum_{j=1}^{n-1}P_{m,j}+\sigma^2\right) \\ \leq& \sum_{j=1}^{n-1}\frac{|h_{m,n}|^2\log_2(e)}{|h_{m,n}|^2\sum_{j=1}^{n-1}P_{m,j}^r+\sigma^2}\left(P_{m,j}-P_{m,j}^r\right) \\ & +\log_2\left(|h_{m,n}|^2\sum_{j=1}^{n-1}P_{m,j}^r+\sigma^2\right) \triangleq \overline{R}_{m,n}^{[e]}, \end{aligned} \tag{25}$$

which is approximated to a concave function. (20a) can be rewritten as

$$R_{m,n}\tau_m \geq \left(\widetilde{R}_{m,n} - \overline{R}_{m,n}^{[e]}\right)\tau_m \geq \delta_{m,n}, 2 \leq n \leq N_m. \tag{26}$$

In particular, when $n = 1$, $R_{m,1}$ needs to satisfy

$$R_{m,1}\tau_m = \log_2\left(1 + \frac{|h_{m,1}|^2 P_{m,1}}{\sigma^2}\right)\tau_m \geq \delta_{m,1}, \tag{27}$$

which is a concave constraint.

Then, according to Proposition 1, (20b) can be transformed as

$$\frac{|h_{m,n}|^2 P_{m,n}}{|h_{m,n}|^2 \sum_{j=1}^{n-1} P_{m,j} + \sigma^2} \geq \eta_{m,n}, \tag{28}$$

which can be rewritten into a convex constraint as

$$P_{m,n} - \eta_{m,n}\sum_{j=1}^{n-1} P_{m,j} \geq \frac{\sigma^2 \eta_{m,n}}{|h_{m,n}|^2}. \tag{29}$$

As a result, the problem (20) can be approximated as

$$\begin{aligned}
(\mathrm{P2}): \max_{\mathbf{P}} & \sum_{m=1}^{M}\sum_{n=1}^{N_m}\left(\widetilde{R}_{m,n} - \overline{R}_{m,n}^{[e]}\right)\tau_m \\
s.t. \ & \left(\widetilde{R}_{m,n} - \overline{R}_{m,n}^{[e]}\right)\tau_m \geq \delta_{m,n}, && \text{(30a)} \\
& P_{m,n} - \eta_{m,n}\sum_{j=1}^{n-1} P_{m,j} \geq \frac{\sigma^2 \eta_{m,n}}{|h_{m,n}|^2}, && \text{(30b)} \\
& 0 < P_{m,1} \leq P_{m,2} \leq ... \leq P_{m,N_m}, && \text{(30c)} \\
& \sum_{n=1}^{N_m} P_{m,n} \leq P_{sum}, n \in \mathbf{\Gamma_m}, m \in \mathbf{\Lambda}, && \text{(30d)}
\end{aligned}$$

which is convex and can be solved by CVX.

C. Location Optimization

Then, with the fixed transmission power $\mathbf{P}$ and duration $\mathbf{T}$, the hovering location can be optimized as

$$\max_{\mathbf{L}} \sum_{m=1}^{M}\sum_{n=1}^{N_m} R_{m,n}\tau_m$$

$$s.t.\ \mathrm{SINR}_{m,n}^{min} \geq \eta_{m,n}, \tag{31a}$$

$$R_{m,n}\tau_m \geq \delta_{m,n}, n \in \mathbf{\Gamma_m}, m \in \mathbf{\Lambda}, \tag{31b}$$

$$\sum_{i=1}^{M} \|\mathbf{L}_{\mathbf{G}(i+1)} - \mathbf{L}_{\mathbf{G}(i)}\| \leq S_{min}. \tag{31c}$$

The objective function, (31a) and (31b) are non-convex with respect to $\mathbf{L}$. First, for (31a), we introduce Proposition 2 to further handle it.

Proposition 2: (31a) can be transformed as

$$\|\mathbf{q}_{m,w} - \mathbf{L}_m\|^2 \leq \rho_0 \frac{P_{m,n} - \eta_{m,n}\sum_{j=1}^{n-1} P_{m,j}}{\eta_{m,n}\sigma^2} - H_0^2, w \leq n, \tag{32}$$

which is convex and can be solved directly.

Proof: $\mathrm{SINR}_{m,n}^{min}$ can be calculated as

$$\begin{aligned}\mathrm{SINR}_{m,n}^{min} &= \min\{\mathrm{SINR}_{m,n}^{w}\}, w \leq n \\ &= \min\{\mathrm{SINR}_{m,n}^{1}, \cdots, \mathrm{SINR}_{m,n}^{n}\}.\end{aligned} \tag{33}$$

To achieve (31a), we have

$$\begin{cases} \mathrm{SINR}_{m,n}^{1} \geq \eta_{m,n}, \\ \mathrm{SINR}_{m,n}^{2} \geq \eta_{m,n}, \\ \quad \cdots \qquad\qquad , \\ \mathrm{SINR}_{m,n}^{n} \geq \eta_{m,n}. \end{cases} \tag{34}$$

$\mathrm{SINR}_{m,n}^{w}$ needs to satisfy

$$\frac{\frac{\rho_0}{H_0^2+\|\mathbf{q}_{m,w}-\mathbf{L}_m\|^2}P_{m,n}}{\frac{\rho_0}{H_0^2+\|\mathbf{q}_{m,w}-\mathbf{L}_m\|^2}\sum_{j=1}^{n-1}P_{m,j}+\sigma^2}\geq\eta_{m,n}, w\leq n, \tag{35}$$

which can be rewritten as

$$\frac{\rho_0 P_{m,n}}{\rho_0\sum_{j=1}^{n-1}P_{m,j}+\sigma^2\left(H_0^2+\|\mathbf{q}_{m,w}-\mathbf{L}_m\|^2\right)}\geq\eta_{m,n}. \tag{36}$$

Thus, we have

$$\eta_{m,n}\sigma^2\big(H_0^2+\|\mathbf{q}_{m,w}-\mathbf{L}_m\|^2\big)\leq\rho_0\left(P_{m,n}-\eta_{m,n}\sum_{j=1}^{n-1}P_{m,j}\right). \tag{37}$$

Accordingly, (32) can be derived. ■

Then, for (31b), we have

$$\begin{cases}\log_2\left(1+\mathrm{SINR}_{m,n}^{1}\right)\tau_m\geq\delta_{m,n},\\ \log_2\left(1+\mathrm{SINR}_{m,n}^{2}\right)\tau_m\geq\delta_{m,n},\\ \quad\cdots\quad,\\ \log_2\left(1+\mathrm{SINR}_{m,n}^{n}\right)\tau_m\geq\delta_{m,n},\end{cases} \tag{38}$$

which is non-convex. For convenience, we define $\log_2\left(1+\mathrm{SINR}_{m,n}^{w}\right)$ as $R_{m,n}^{w}$. To perform the approximation, we rewrite $R_{m,n}^{w}$ as

$$\begin{aligned}R_{m,n}^{w}&=\log_2\left(1+\frac{|h_{m,w}|^2P_{m,n}}{|h_{m,w}|^2\sum_{j=1}^{n-1}P_{m,j}+\sigma^2}\right)\\&=\hat{R}_{m,n}^{w}-\check{R}_{m,n}^{w}, w\leq n, m\in\mathbf{\Lambda},\end{aligned} \tag{39}$$

where $\hat{R}^w_{m,n}$ and $\check{R}^w_{m,n}$ can be expressed as

$$\begin{cases} \hat{R}^w_{m,n} = \log_2\left(\dfrac{\rho_0}{H_0^2+\|\mathbf{q}_{m,w}-\mathbf{L}_m\|^2}\sum\limits_{j=1}^{n} P_{m,j}+\sigma^2\right), \\ \check{R}^w_{m,n} = \log_2\left(\dfrac{\rho_0}{H_0^2+\|\mathbf{q}_{m,w}-\mathbf{L}_m\|^2}\sum\limits_{j=1}^{n-1} P_{m,j}+\sigma^2\right). \end{cases} \tag{40}$$

Regarding $\|\mathbf{q}_{m,w}-\mathbf{L}_m\|^2$ as a variable, we have that both $\hat{R}^w_{m,n}$ and $\check{R}^w_{m,n}$ are convex. Thus, we need to first transform $\hat{R}^w_{m,n}$ into a concave one. Define L^r_m as the hovering location in the r-th iteration. We can obtain the first-order expansion of $\hat{R}^w_{m,n}$ at $\|\mathbf{q}_{m,w}-\mathbf{L}^r_m\|^2$ by Lemma 1 as

$$\begin{aligned} \hat{R}^w_{m,n} &= \log_2\left(\frac{\rho_0}{H_0^2+\|\mathbf{q}_{m,w}-\mathbf{L}_m\|^2}\sum_{j=1}^{n} P_{m,j}+\sigma^2\right) \\ &\geq -C^w_{m,n}\left(\|\mathbf{q}_{m,w}-\mathbf{L}_m\|^2-\|\mathbf{q}_{m,w}-\mathbf{L}^r_m\|^2\right) \\ &\quad +\log_2\left(\frac{\rho_0}{H_0^2+\|\mathbf{q}_{m,w}-\mathbf{L}^r_m\|^2}\sum_{j=1}^{n} P_{m,j}+\sigma^2\right) \\ &\triangleq \dot{R}^w_{m,n}, \end{aligned} \tag{41}$$

which is concave with respect to $\mathbf{L}$. $C^w_{m,n}$ can be expressed as

$$C^w_{m,n} = \frac{\dfrac{\rho_0\log_2(e)}{(H_0^2+\|\mathbf{q}_{m,w}-\mathbf{L}^r_m\|^2)^2}\sum\limits_{j=1}^{n} P_{m,j}}{\dfrac{\rho_0}{H_0^2+\|\mathbf{q}_{m,w}-\mathbf{L}^r_m\|^2}\sum\limits_{j=1}^{n} P_{m,j}+\sigma^2}. \tag{42}$$

Accordingly, $R^w_{m,n}$ can be approximated as

$$R^w_{m,n} \geq \dot{R}^w_{m,n} - \check{R}^w_{m,n}, \tag{43}$$

which is still non-concave with respect to $\mathbf{L}$ due to $\check{R}^w_{m,n}$. Therefore, we introduce the slack variable $V_{m,w}$, which satisfies

$$V_{m,w} \leq \|\mathbf{q}_{m,w}-\mathbf{L}_m\|^2, w \in \mathbf{\Gamma_m}, m \in \mathbf{\Lambda}. \tag{44}$$

This is a non-convex constraint due to $\|\mathbf{q}_{m,w} - \mathbf{L}_m\|^2$. Thus, we approximate it through the first-order expansion at L_m^r as

$$\|\mathbf{q}_{m,w}-\mathbf{L}_m\|^2 \geq \|\mathbf{q}_{m,w}-\mathbf{L}_m^r\|^2+2(\mathbf{q}_{m,w}-\mathbf{L}_m^r)^\dagger(\mathbf{L}_m^r-\mathbf{L}_m). \tag{45}$$

As a result, for (44), we have

$$V_{m,w} \leq \|\mathbf{q}_{m,w} - \mathbf{L}_m^r\|^2 + 2(\mathbf{q}_{m,w} - \mathbf{L}_m^r)^\dagger(\mathbf{L}_m^r - \mathbf{L}_m). \tag{46}$$

Substituting $\|\mathbf{q}_{m,w} - \mathbf{L}_m\|^2$ by $V_{m,w}$, $\check{R}_{m,n}$ can be reformulated as

$$\check{R}_{m,n}^w \leq \log_2\left(\frac{\rho_0}{H_0^2 + V_{m,w}}\sum_{j=1}^{n-1} P_{m,j} + \sigma^2\right) \triangleq \ddot{R}_{m,n}^w, \tag{47}$$

which is convex.

Finally, $R_{m,n}^w$ can be approximated to a concave function, which satisfies

$$R_{m,n}^w \tau_m \geq \left(\dot{R}_{m,n}^w - \ddot{R}_{m,n}^w\right)\tau_m \geq \delta_{m,n}. \tag{48}$$

From the above derivation, all the constraints have been transformed into convex ones. In addition, the sum throughput can be expressed as

$$R_{sum}=\sum_{m=1}^{M}\sum_{n=1}^{N_m}\min\{\dot{R}_{m,n}^1-\ddot{R}_{m,n}^1, \cdots, \dot{R}_{m,n}^n-\ddot{R}_{m,n}^n\}\tau_m, \tag{49}$$

which is concave. Thus, the location optimization can be transformed as

$$(\mathrm{P3}): \max_{\mathbf{L},\mathrm{V_{m,w}}} \; R_{sum}$$

$$s.t. \;\; \left(\dot{R}_{m,n}^w-\ddot{R}_{m,n}^w\right)\tau_m \geq \delta_{m,n}, \tag{50a}$$

$$\|\mathbf{q}_{m,w}-\mathbf{L}_m\|^2 \leq \rho_0 \frac{P_{m,n}-\eta_{m,n}\sum_{j=1}^{n-1}P_{m,j}}{\eta_{m,n}\sigma^2} - H_0^2, \tag{50b}$$

$$\sum_{i=1}^{M} \| \mathbf{L}_{\mathbf{G}(i+1)} - \mathbf{L}_{\mathbf{G}(i)} \| \leq S_{min}, \tag{50c}$$

$$V_{m,w} \geq 0, w \leq n \in \mathbf{\Gamma_m}, m \in \mathbf{\Lambda}, \tag{50d}$$

$$V_{m,w} \leq \|\mathbf{q}_{m,w}-L_m^r\|^2+2(\mathbf{q}_{m,w}-\mathbf{L}_m^r)^\dagger(\mathbf{L}_m^r-\mathbf{L}_m), \tag{50e}$$

which is convex and can be solved via CVX. Meanwhile, the decoding order should be updated according to the results.

D. Duration Optimization

The transmission duration $\mathbf{T}$ is optimized with $\mathbf{P}$ and $\mathbf{L}$ obtained by solving $(\mathrm{P2})$ and $(\mathrm{P3})$. Thus, we have

$$(\mathrm{P4}): \max_{\mathbf{T}} \sum_{m=1}^{M}\sum_{n=1}^{N} R_{m,n}\tau_m$$

$$s.t. \sum_{m=1}^{M} \tau_m \leq T_0 - T_S, \tag{51a}$$

$$R_{m,n}\tau_m \geq \delta_{m,n}, n \in \mathbf{\Gamma_m}, m \in \mathbf{\Lambda}. \tag{51b}$$

To obtain the flying duration T_S, assume that the maximum speed of UAV is ν. During the flight, the UAV first accelerates to reach the maximum speed, then keeps the constant velocity motion, and finally decelerates to the next hovering location. Thus, the flying duration of UAV T_S can be calculated as

$$T_S = \frac{S_{min} - S_\alpha}{\nu} + T_\alpha, \tag{52}$$

where S_α and T_α are the sum distance and time during the accelerating and decelerating with the same acceleration α. Meanwhile, S_{min} can be updated in each iteration according to the optimized locations. Thus, S_α and T_α can be expressed as

$$\begin{cases} S_\alpha = 2M \cdot \dfrac{\nu^2}{2\alpha}, \\ T_\alpha = 2M \cdot \dfrac{\nu}{\alpha}. \end{cases} \tag{53}$$

As a result, for (51a), we have

$$\sum_{m=1}^{M} \tau_m \leq T_0 - \frac{S_{min}}{\nu} - \frac{M \cdot \nu}{\alpha}. \tag{54}$$

Thus, $(\mathrm{P4})$ is a standard linear programming, which can be solved by CVX directly.

Algorithm 3 - Alternating Optimization Algorithm for $(\mathrm{P1})$

1: **Initialization**: The initial transmission duration of UAV in each cluster τ_m^0 is set to $(T_0 - T_S)/M$. The initial locations are initialized as the centroids of each cluster, $L_m^0 = \sum_{n=1}^{N_m} q_{m,n}/N_m$. The initial power is allocated to satisfy the requirements of users. Set the initial index of iterations as $k = 0$.
2: **Repeat**
3: Set the initial index of iterations as $r = 0$.
4: **Repeat**
5: Solve $(\mathrm{P2})$, and obtain the optimal power P^{r+1}.
6: Solve $(\mathrm{P3})$, and obtain the optimal location L^{r+1}.
7: Adjust the decoding order in each cluster via L^{r+1}.
8: Update: $r = r + 1$.
9: **Until P** and **L** are convergent.
10: Solve $(\mathrm{P4})$, obtain the optimized duration T^{k+1}.
11: Update: $k = k + 1$.
12: **Until** convergence.
13: Output: **P**, **L**, **T** and the throughput.

E. Proposed Algorithm

Accordingly, the problem $(\mathrm{P1})$ have been divided into three subproblems, which are transformed into convex ones. Thus, we propose an iterative algorithm to solve the problem, summarized as Algorithm 3, with its convergence proved as follows.

Assume that the throughput in the r-th inner iteration and the k-th outer iteration is $R_{sum}(P^r, L^r, T^k)$. By Step 5 and Step 6 in Algorithm 3, we can obtain better power allocation P^{r+1} and hovering location L^{r+1}, and have

$$R_{sum}(P^{r+1}, L^{r+1}, T^k) \geq R_{sum}(P^r, L^r, T^k). \tag{55}$$

In Step 7, the decoding order is updated, and the throughput cannot always decrease. After Step 10, the duration is re-allocated via P^r and L^r. The throughput cannot decrease. Thus, we

have

$$R_{sum}(P^r, L^r, T^{k+1}) \geq R_{sum}(P^r, L^r, T^k). \tag{56}$$

Since the resource is limited, the throughput has a specific upper bound, and cannot always decrease. Therefore, Algorithm 3 is convergent.

In Algorithm 3, $(\mathrm{P2})$ and $(\mathrm{P3})$ are solved by SCA, the computational complexity of which is about the number of iterations and optimization variables [33]. Since there are K users in the network, both $(\mathrm{P2})$ and $(\mathrm{P3})$ have K variables. Meanwhile, $(\mathrm{P4})$ is a linear programming, whose computational complexity can be denoted as $\mathcal{O}\left(M\left(K+1\right)^2\right)$. Thus, the overall computational complexity of Algorithm 3 can be calculated as

$$\mathcal{O}\left(I_2\left(2I_1K^3 + M\left(K+1\right)^2\right)\right), \tag{57}$$

where I_1 and I_2 represent the number of inner and outer iterations, respectively.

V. Simulation Results and Discussion

In this section, simulation results are presented to demonstrate the effectiveness of the proposed scheme. The parameters are set as follows. The power of AWGN σ^2 is set as -110 dBm. In addition, we set the reference channel coefficient ρ_0 as -60 dB. Assume that all the users have the same QoS requirement and throughput threshold, i.e., $\eta_{m,n} = \eta_0, \delta_{m,n} = \delta_0 = 3$ bit/Hz, $n \in \mathbf{\Gamma_m}, m \in \mathbf{\Lambda}$. To establish LoS links, the altitude of UAV H_0 is set to 150 m. Meanwhile, the maximum speed and acceleration of UAV are set as $\nu = 8$ m/s and $\alpha = 4$ m/s^2, respectively.

To prove the effectiveness of Algorithm 2, the proposed GA algorithm is compared with ES in Table 1. In the simulation, the mutation probability ϱ is set to 0.4. Furthermore, to achieve better performance, the number of individuals Z needs to increase with M. Since the results

TABLE I

PERFORMANCE COMPARISON OF GA AND ES

	Z	β	S_{min} (km)	Complexity
ES with 7 clusters			3.3686	$\mathcal{O}$(5040)
GA with 7 clusters	30	50	3.5007	$\mathcal{O}$(73500)
ES with 8 clusters			3.9018	$\mathcal{O}$(40320)
GA with 8 clusters	40	50	4.0382	$\mathcal{O}$(128000)
ES with 9 clusters			3.9691	$\mathcal{O}$(362880)
GA with 9 clusters	40	50	4.2639	$\mathcal{O}$(162000)
ES with 10 clusters			4.2669	$\mathcal{O}$(3628800)
GA with 10 clusters	50	50	4.6848	$\mathcal{O}$(250000)
ES with 11 clusters			4.6234	$\mathcal{O}$(39916800)
GA with 11 clusters	50	50	4.9502	$\mathcal{O}$(302500)

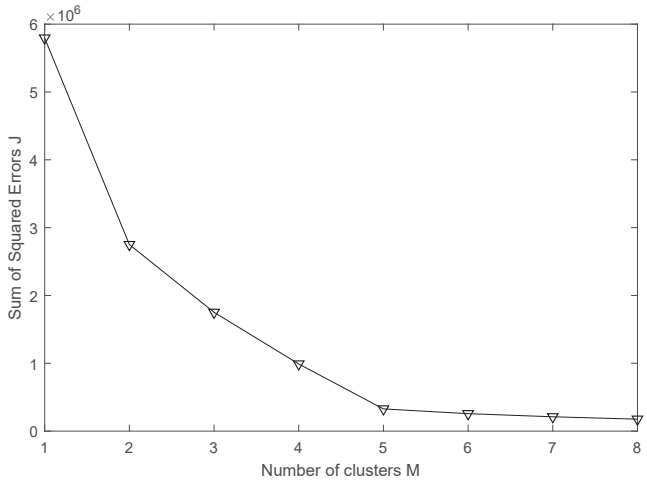

Fig. 2. The value of $\mathcal{J}$ with M increasing in the K-means algorithm when there are 19 users.

obtained by GA are not fixed, the GA algorithm is performed 100 times, and the average results are shown. From the comparison, we can find that the computational complexity of GA is much less than that of ES when the number of clusters M is no smaller than 9. Furthermore, the results obtained by GA are very close to those by ES. Thus, we can adopt the ES when $M < 9$, otherwise, the GA-based algorithm is performed to optimize the UAV routing.

From Fig. 2 to Fig. 7, we first consider the NOMA-UAV network with 19 users, which can

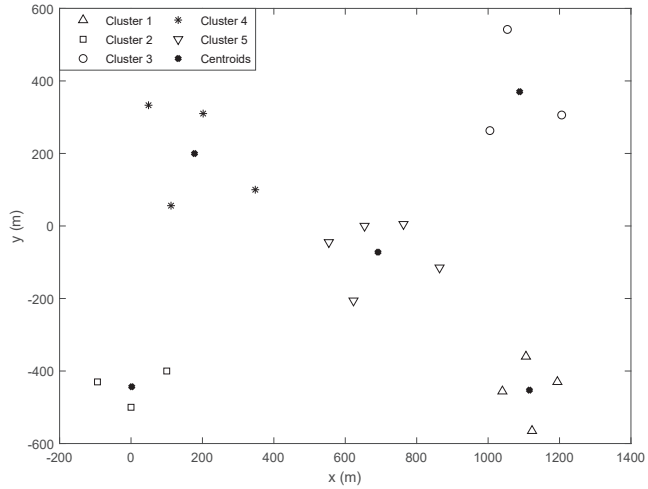

Fig. 3. User clustering results via the K-means algorithm with 19 users.

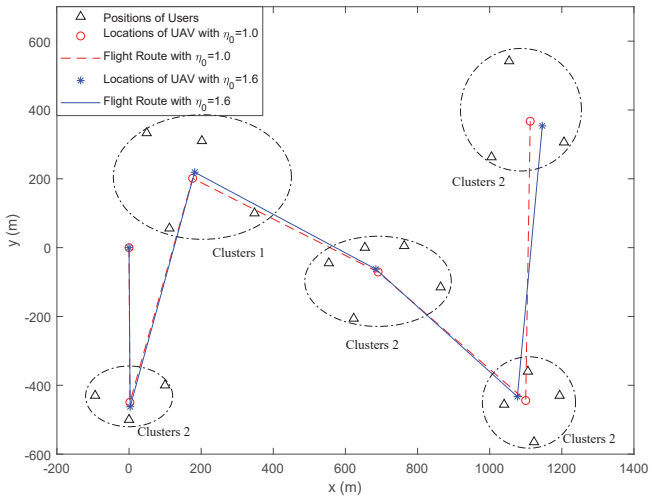

Fig. 4. Optimal routing and hovering locations of UAV with different QoS requirements.

be divided into 5 clusters by Algorithm 1. To guarantee that the UAV can complete all the tasks, the whole duration T_0 is set as 415 s.

Fig. 2 and Fig. 3 show the clustering results of the K-means algorithm. The values of $\mathcal{J}$ with the increase of M are first shown in Fig. 2. From the results, we can find that the value of $\mathcal{J}$ sharply decreases before $M = 5$, after which the trend gets stable. According to the elbow method, the suitable number of clusters M is 5. The result of user clustering is presented in Fig.

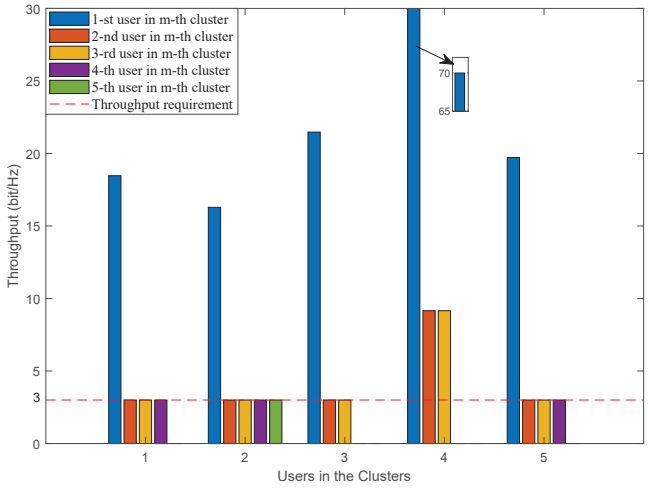

Fig. 5. Throughput of each user with $\eta_0 = 1.0$ when there are 19 users in the network.

3. From the results, we can see that the distributed randomly users can be effectively grouped into 5 clusters by the K-means algorithm.

Fig. 4 shows the optimal routing and hovering locations of UAV with different QoS requirements. Since the number of clusters is 5, we adopt ES to search the optimal routing. Meanwhile, the total transmission power P_{sum} of UAV is set as 0.2 W. From the results, we can see that the UAV routing and locations can be effectively optimized. Furthermore, we find that the optimal UAV locations get closer to the users with better channels when the QoS threshold of users η_0 increases. This is because the users with worse channels will be allocated more power to achieve higher QoS. Due to the limited power, the users with better channels will be allocated less. Therefore, the locations of UAV get closer to the users with better channels to compensate for their transmission power.

In Fig. 5 and Fig. 6, we set $\eta_0 = 1.0$. The throughput of each user is first shown in Fig. 5. We can find that the throughput requirement of each user can be satisfied by the proposed scheme. Furthermore, we show the sum rate and duration allocated for each cluster in Fig. 6. From the results in Fig. 5 and Fig. 6, we can find that the resource allocated to the users with

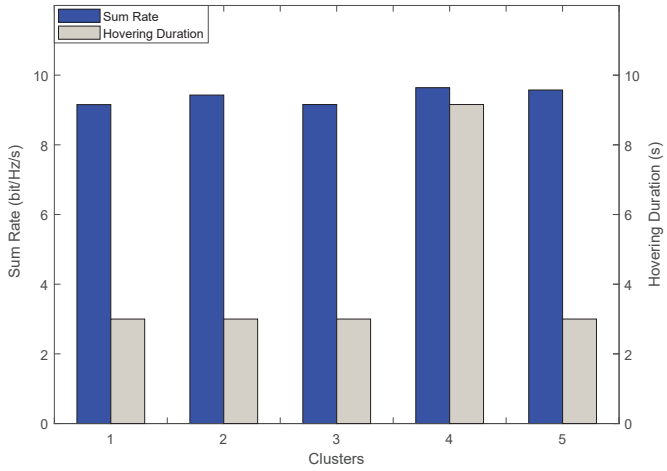

Fig. 6. Sum rate and hovering duration for the 5 clusters with $\eta_0 = 1.0$.

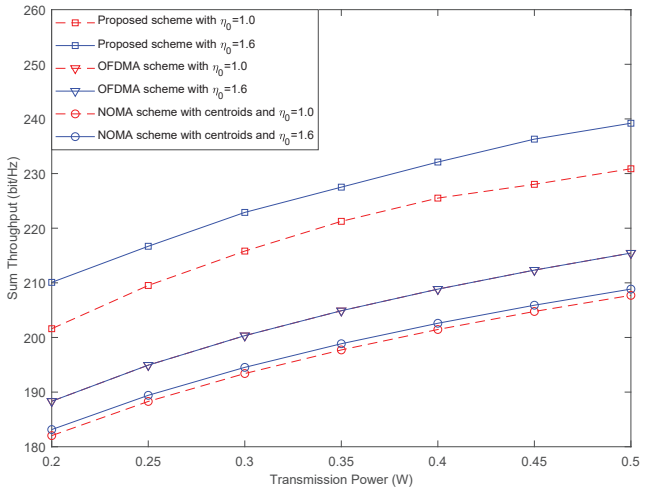

Fig. 7. Sum throughput of the proposed scheme and benchmarks with different the transmission power.

worse channels can just satisfy their requirements, and more resource trends to be allocated to the user with the best channel in each cluster to maximize the sum throughput.

The sum throughput of the proposed scheme is compared with benchmarks in Fig. 7. The first benchmark is the OFDMA scheme, which can be solved by SCA. The second benchmark is the NOMA scheme, where the hovering locations are the centroids of clusters determined by the method in [25]. The results show that the proposed scheme has much better performance than

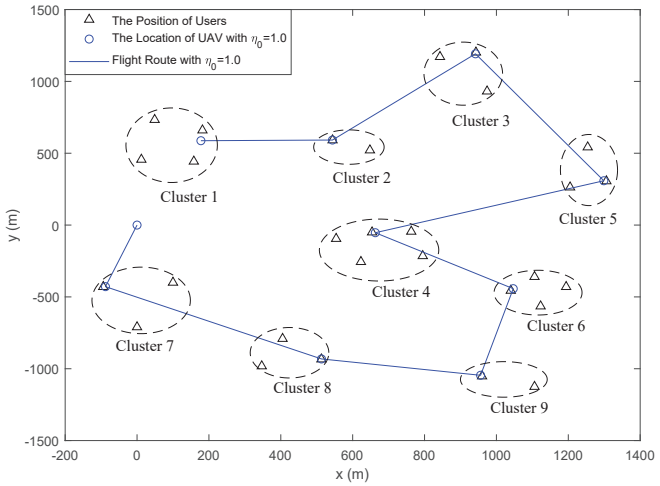

Fig. 8. The optimal locations and routing of UAV with $\eta_0 = 1.0$ for the case of 29 users in 9 clusters.

both the two benchmarks. Furthermore, in the two schemes with NOMA, the sum throughput is higher with stricter QoS requirement. This is because higher QoS means higher achievable rate, and less transmission duration is needed for the clusters with worse channels. In this way, more transmission duration can be allocated to the clusters with the better channels, and the sum throughput can be improved. On the other hand, the throughput of OFDMA is not affected by QoS requirements, because the transmission power is almost equally distributed among users. The SINR can reach a high level for each user, which exceed the QoS requirements.

After that, we consider the NOMA-UAV network of 29 users to verify the effectiveness of the proposed scheme with more users. We set the QoS threshold η_0 and T_0 to 1.0 and 489 s, respectively. The positions of users, optimized routing and hovering locations of UAV are shown in Fig. 8. In the network, the users are divided into 9 clusters by Algorithm 1. Accordingly, the optimal routing of UAV can be obtained by GA in Algorithm 2. From the results, we can find that the GA-based algorithm can effectively optimize the UAV routing. Then, we show the throughput of each user when there are 29 users in Fig. 9. From the result, we can find that the proposed scheme can satisfy the throughput threshold of 3 bit/Hz for all the users, and

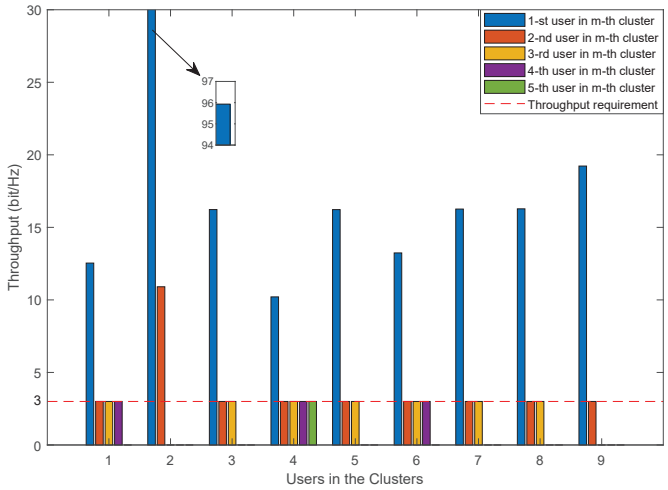

Fig. 9. Throughput of each user with $\eta_0 = 1.0$ when there are 29 users in the network.

the throughput of the 2nd cluster highly exceeds the threshold. This is because the 2nd cluster has the best channel condition, and more resource will be allocated to it to maximize the sum throughput.

VI. Conclusion

In this paper, we have proposed a resource allocation scheme to maximize the sum throughput of the NOMA-UAV network with multiple clusters. To satisfy the QoS requirements of all users, we first propose a K-means algorithm to group the users into M clusters. In addition, GA is adopted to obtain the optimal routing of UAV. Based on the optimal clusters and routing, we jointly optimize the transmission power, hovering locations and transmission duration of UAV to maximize the sum throughput, which is a non-convex problem. We divide it into three subproblems including two non-convex subproblems and a linear programming one. Thus, we adopt SCA to transform the non-convex subproblems into convex ones. Finally, an iterative algorithm is proposed to solve the resource allocation problem. Simulation results show that the proposed scheme is effective and has better performance than the benchmarks.

REFERENCES

[1] Q. Huang, W. Wang, W. Lu, N. Zhao, A. Nallanathan, and X. Wang, "Throughput maximization for multi-cluster NOMA-UAV networks," in *Proc. IEEE GLOBECOM'22*, pp. 1–6, Rio de Janeiro, Brazil, Dec. 2022.

[2] Y. Zeng, R. Zhang, and T. J. Lim, "Wireless communications with unmanned aerial vehicles: opportunities and challenges," *IEEE Commun. Mag.*, vol. 54, no. 5, pp. 36–42, May, 2016.

[3] N. Zhao, W. Lu, M. Sheng, Y. Chen, J. Tang, F. R. Yu, and K.-K. Wong, "UAV-assisted emergency networks in disasters," *IEEE Wireless Commun.*, vol. 26, no. 1, pp. 45–51, Feb. 2019.

[4] A. A. Khuwaja, Y. Chen, N. Zhao, M.-S. Alouini, and P. Dobbins, "A survey of channel modeling for UAV communications," *IEEE Commun. Surveys Tuts.*, vol. 20, no. 4, pp. 2804–2821, 4th Quart. 2018.

[5] L. Gupta, R. Jain, and G. Vaszkun, "Survey of important issues in UAV communication networks," *IEEE Commun. Surveys Tuts.*, vol. 18, no. 2, pp. 1123–1152, 2nd Quart. 2016.

[6] X. Lin, V. Yajnanarayana, S. D. Muruganathan, S. Gao, H. Asplund, H.-L. Maattanen, M. Bergstrom, S. Euler, and Y.-P. E. Wang, "The sky is not the limit: LTE for unmanned aerial vehicles," *IEEE Commun. Mag.*, vol. 56, no. 4, pp. 204–210, Apr. 2018.

[7] Y. Zeng, Q. Wu, and R. Zhang, "Accessing from the sky: A tutorial on UAV communications for 5G and beyond," *Proc. IEEE*, vol. 107, no. 12, pp. 2327–2375, Dec. 2019.

[8] Y. Zeng, R. Zhang, and T. J. Lim, "Throughput maximization for UAV-enabled mobile relaying systems," *IEEE Trans. Commun.*, vol. 64, no. 12, pp. 4983–4996, Dec. 2016.

[9] Q. Wu, Y. Zeng, and R. Zhang, "Joint trajectory and communication design for multi-UAV enabled wireless networks," *IEEE Trans. Wireless Commun.*, vol. 17, no. 3, pp. 2109–2121, Mar. 2018.

[10] H. Wang, G. Ren, J. Chen, G. Ding, and Y. Yang, "Unmanned aerial vehicle-aided communications: Joint transmit power and trajectory optimization," *IEEE Wireless Commun. Lett.*, vol. 7, no. 4, pp. 522–525, Aug. 2018.

[11] Q. Wu and R. Zhang, "Common throughput maximization in UAV-enabled OFDMA systems with delay consideration," *IEEE Trans. Commun.*, vol. 66, no. 12, pp. 6614–6627, Dec. 2018.

[12] K. Meng, Q. Wu, S. Ma, W. Chen, and T. Q. S. Quek, "UAV trajectory and beamforming optimization for integrated periodic sensing and communication," *IEEE Wireless Commun. Lett.*, vol. 11, no. 6, pp. 1211–1215, Jun. 2022.

[13] Z. Ding, X. Lei, G. K. Karagiannidis, R. Schober, J. Yuan, and V. K. Bhargava, "A survey on non-orthogonal multiple access for 5G networks: Research challenges and future trends," *IEEE J. Select. Areas Commun.*, vol. 35, no. 10, pp. 2181–2195, Oct. 2017.

[14] S. M. R. Islam, N. Avazov, O. A. Dobre, and K.-s. Kwak, "Power-domain non-orthogonal multiple access (NOMA) in 5G systems: Potentials and challenges," *IEEE Commun. Surveys Tuts.*, vol. 19, no. 2, pp. 721–742, 2nd Quart. 2017.

[15] Y. Liu, S. Zhang, X. Mu, Z. Ding, R. Schober, N. Al-Dhahir, E. Hossain, and X. Shen, "Evolution of NOMA toward next generation multiple access (NGMA) for 6G," *IEEE J. Select. Areas Commun.*, vol. 40, no. 4, pp. 1037–1071, Apr. 2022.

[16] Z. Ding, P. Fan, G. K. Karagiannidis, R. Schober, and H. V. Poor, "NOMA assisted wireless caching: Strategies and performance analysis," *IEEE Trans. Commun.*, vol. 66, no. 10, pp. 4854–4876, Oct. 2018.

[17] Z. Chen, Z. Ding, X. Dai, and R. Zhang, "An optimization perspective of the superiority of NOMA compared to conventional OMA," *IEEE Trans. Signal Process.*, vol. 65, no. 19, pp. 5191–5202, Oct. 2017.

[18] C.-L. Wang, J.-Y. Chen, and Y.-J. Chen, "Power allocation for a downlink non-orthogonal multiple access system," *IEEE Wireless Commun. Lett.*, vol. 5, no. 5, pp. 532–535, Oct. 2016.

[19] Z. Yang, C. Pan, W. Xu, Y. Pan, M. Chen, and M. Elkashlan, "Power control for multi-cell networks with non-orthogonal multiple access," *IEEE Trans. Wireless Commun.*, vol. 17, no. 2, pp. 927–942, Feb. 2018.

[20] Z. Xiao, L. Zhu, J. Choi, P. Xia, and X.-G. Xia, "Joint power allocation and beamforming for non-orthogonal multiple access (NOMA) in 5G millimeter wave communications," *IEEE Trans. Wireless Commun.*, vol. 17, no. 5, pp. 2961–2974, May 2018.

[21] L. Zhu, J. Zhang, Z. Xiao, X. Cao, D. O. Wu, and X.-G. Xia, "Joint power control and beamforming for uplink non-orthogonal multiple access in 5G millimeter-wave communications," *IEEE Trans. Wireless Commun.*, vol. 17, no. 9, pp. 6177–6189, Sept. 2018.

[22] S. Feng, T. Bai, and L. Hanzo, "Joint power allocation for the multi-user NOMA-downlink in a power-line-fed VLC network," *IEEE Trans. Veh. Technol.*, vol. 68, no. 5, pp. 5185–5190, May 2019.

[23] N. Zhao, X. Pang, Z. Li, Y. Chen, F. Li, Z. Ding, and M.-S. Alouini, "Joint trajectory and precoding optimization for UAV-assisted NOMA networks," *IEEE Trans. Commun.*, vol. 67, no. 5, pp. 3723–3735, May 2019.

[24] Y. Liu, Z. Qin, Y. Cai, Y. Gao, G. Y. Li, and A. Nallanathan, "UAV communications based on non-orthogonal multiple access," *IEEE Wireless Commun.*, vol. 26, no. 1, pp. 52–57, Feb. 2019.

[25] X. Liu, J. Wang, N. Zhao, Y. Chen, S. Zhang, Z. Ding, and F. R. Yu, "Placement and power allocation for NOMA-UAV networks," *IEEE Wireless Commun. Lett.*, vol. 8, no. 3, pp. 965–968, Jun. 2019.

[26] R. Zhang, X. Pang, J. Tang, Y. Chen, N. Zhao, and X. Wang, "Joint location and transmit power optimization for NOMA-UAV networks via updating decoding order," *IEEE Wireless Commun. Lett.*, vol. 10, no. 1, pp. 136–140, Jan. 2021.

[27] W. Feng, N. Zhao, S. Ao, J. Tang, X. Zhang, Y. Fu, D. K. C. So, and K.-K. Wong, "Joint 3D trajectory and power optimization for UAV-aided mmwave MIMO-NOMA networks," *IEEE Trans. Commun.*, vol. 69, no. 4, pp. 2346–2358, Apr. 2021.

[28] M. Katwe, K. Singh, P. K. Sharma, C.-P. Li, and Z. Ding, "Dynamic user clustering and optimal power allocation in UAV-assisted full-duplex hybrid NOMA system," *IEEE Trans. Wireless Commun.*, vol. 21, no. 4, pp. 2573–2590, Apr. 2022.

[29] C. Pan, H. Ren, Y. Deng, M. Elkashlan, and A. Nallanathan, "Joint blocklength and location optimization for URLLC-enabled UAV relay systems," *IEEE Commun. Lett.*, vol. 23, no. 3, pp. 498–501, Jan. 2019.

[30] J. Cui, Z. Ding, P. Fan, and N. Al-Dhahir, "Unsupervised machine learning-based user clustering in millimeter-wave-NOMA systems," *IEEE Trans. Wireless Commun.*, vol. 17, no. 11, pp. 7425–7440, Mar. 2019.

[31] R. Tibshirani, G. Walther, and T. Hastie, "Estimating the number of clusters in a data set via the gap statistic," *Statist. Methodol.*, vol. 63, no. 2, pp. 411–423, Jan. 2002.

[32] T. Li and Z. Ge, "A multiple QoS anycast routing algorithm based adaptive genetic algorithm," *Proc. 3d Int. Conf. Genetic Evol. Comput.*, pp. 89–92, Oct. 2009.

[33] C. Zhan and Y. Zeng, "Aerialground cost tradeoff for multi-UAV-enabled data collection in wireless sensor networks," *IEEE Trans. Commun.*, vol. 68, no. 3, pp. 1937–1950, Mar. 2020.